via receptor protein tyrosine kinases such as EGF receptor (EGFR) and FGF receptor. Ras can associate with the plasma membrane by virtue of lipid modifications at its COOH terminus (10). This recruitment to the plasma membrane transduces Ras from an inactive form (GDP-Ras) to an active form (GTP-Ras), and is essential for activation by growth factors (10). GTP-Ras interacts with Raf-1, localizing the latter to the plasma membrane where it becomes activated by several kinases and phosphatases (9). Activated Raf-1 then induces the sequential activation of MEK1/2 and ERK1/2 in a phosphorylation-dependent manner. Activated ERK1/2 then translocate from the cytoplasm to the nucleus and activate a number of transcription factors associated with cell cycle progression, survival, development, and differentiation (9). ERK1/2 also transduce signals to RSKs and thereby positively regulate cell cycle progression by promoting the cyclic AMP response element binding protein–dependent transactivation of cyclin A and cyclin D1, and by inhibiting the nuclear translocation of the cyclin-dependent kinase inhibitor, $p27^{Kip1}$ (11–13). Hence, the MEK-ERK-RSK pathway plays a central role during cell growth and survival.

In our previous studies, we have shown that estrogens down-regulate both P-gp and BCRP expression levels (14, 15). We have also further shown that the down-regulation of BCRP by 17β-estradiol (E_2) is dependent on the posttranscriptional inhibition of protein biosynthesis, but not on protein degradation (14). It has been shown by others that phosphatidylinositol 3-OH kinase (PI3K) inhibitors also down-regulate BCRP expression levels (16). Studies of small molecules or physiologic compounds that suppress ABC transporter protein expression are thus now ongoing. In our present study, we examine the effects of several signal transduction inhibitors upon the expression levels of P-gp, and find that U0126, PD98059, *ERK* small interfering RNA (siRNA), and *RSK* siRNA inhibit P-gp expression. Moreover, U0126 down-regulate P-gp expression by promoting its degradation, but does not affect its biosynthesis. Our present findings thus provide an increased understanding of P-gp biosynthesis and degradation and reveal potential new strategies for the circumvention of P-gp–mediated drug resistance.

Materials and Methods

Reagents

U0126 and PD98059 were purchased from Cell Signaling Technology. 17-Allylamino-17-demethoxygeldanamycin (17-AAG) was purchased from Alomone Labs. Rapamycin, SP600125, EGF, bFGF, and rhodamine123 were purchased from Sigma. FTI-277, LY294002, and SB203580 were obtained from Calbiochem. Paclitaxel was obtained from Bristol-Myers Squibb.

Antibodies for Western blotting were purchased as follows: anti-MDR1+3 monoclonal antibody (C219; Zymed); anti-glyceraldehyde-3-phosphate dehydrogenase (GAPDH) monoclonal antibody (Chemicon); anti-p44/p42, anti–phospho-p44/p42 (Thr^{202}/Tyr^{204}), anti-Akt, and anti–phospho-Akt (Ser^{473}) polyclonal antibodies and anti–phospho-EGFR (Tyr^{1068}) monoclonal antibody (Cell Signaling Technology); anti-EGFR monoclonal antibody (Santa Cruz Biotechnology); and anti–poly(ADP-ribose) polymerase (PARP) p85 fragment polyclonal antibody (Promega).

Cells

The human cancer cell lines used in this study were obtained from the National Cancer Institute (Bethesda, MD). SW620-14 cells were isolated from human colorectal tumor SW620 cells by limiting dilution. The *MDR1*-transduced human breast cancer cell lines MCF-7/MDR and MDA-MB-231/MDR were established by transduction with the HaMDR retrovirus as described previously (15). MDA-MB-231 cells were transduced with the Ha3HisMDR retrovirus harboring 3′-His–tagged human *MDR1* cDNA. The transduced cells were selected with 3 nmol/L vincristine for 10 days and the resulting mixed population was designated MDA-MB-231/3HisMDR. All cells were cultured in the growth medium consisting of 93% DMEM and 7% fetal bovine serum (FBS) at 37°C in 5% CO_2.

Western Blotting and Immunoprecipitation

Cell membrane and cytoplasmic fractions were prepared from cells in lysis buffer [0.2% NP40, 10% glycerol, 137 mmol/L NaCl, 20 mmol/L Tris-Cl (pH 7.5), 1.5 mol/L $MgCl_2$, 1 mmol/L EDTA (pH 8.0), 50 mmol/L NaF, 1 mmol/L Na_3PO_4, 12 mmol/L β-glycerophosphate, 1 mmol/L phenylmethylsulfonyl fluoride, 1 mmol/L aprotinin]. For immunoprecipitation of 3HisP-gp from MDA-MB-231/3HisMDR cells, 500 μg of protein were incubated with Ni-NTA agarose (Qiagen) for 2 h on ice with occasional tapping. The immunocomplexes precipitated with the Ni-NTA agarose were then washed five times with ice-cold wash buffer [1 mol/L Tris-Cl (pH 7.5), 1 mol/L NaCl, 1% Triton X-100]. Whole-cell lysates were prepared with SDS-containing lysis buffer [1% SDS, 10% glycerol, and 100 mmol/L Tris-Cl (pH 7.5)]. All cell lysates and immunoprecipitates were solubilized with sample buffer [2% SDS, 50 mmol/L Tris-HCl (pH 8.0), 0.2% bromophenol blue, 5% 2-mercaptoethanol] with boiling for 5 min at 100°C, separated by SDS-PAGE, and then transferred onto nitrocellulose membranes. The membranes were incubated with primary antibodies following by peroxidase-conjugated sheep anti-mouse or anti-rabbit secondary antibodies (Amersham Biosciences Corp.). Bands were visualized with the ECL (enhanced chemiluminescence) Plus detection kit (Amersham Biosciences Corp.).

siRNA Transfection

Nonsilencing control siRNA were purchased from Qiagen. *ERK* siRNA was obtained from Cell Signaling Technology and comprises a mixture of *ERK1* and *ERK2* siRNAs. *RSK* siRNA was purchased from Qiagen and was composed of *RSK1*, *RSK2*, and *RSK3* siRNAs. Cells were transfected with these siRNAs using LipofectAMINE 2000 (Invitrogen), according to the manufacturer's instructions.

Plasmid DNAs and Transfection

Human wild-type (WT) *H-Ras, Raf-1, MEK1, MEK2, ERK1, ERK2, RSK1, RSK2, p85α* regulatory subunit of *PI3K, akt1*, and *phosphatase and tensin homologue deleted in chromosome 10* (*PTEN*) cDNAs were generated by PCR with a Human Liver BD Marathon-Ready cDNA (BD Biosciences Clontech) as the template. The PCR products were then digested and cloned into the pFLAG-CMV-2 vector (Sigma). Mutant *PTEN* cDNA was constructed by the substitution of Cys^{124} with Ser of *PTEN* (WT) using a QuickChange Site-Directed Mutagenesis kit (Stratagene). Cells were transfected with these plasmid DNAs using LipofectAMINE 2000 (Invitrogen).

Semiquantitative Reverse Transcription-PCR of *MDR1*

Cells were treated with either 10 μmol/L U0126 or 100 μg/L EGF, and total RNA was then extracted using an RNeasy kit (Qiagen). Reverse transcription-PCR (RT-PCR) was done using RNA LA PCR kit (Takara) as described previously (15). Real-time RT-PCR was done using SYBR Green PCR Master Mix and RT-PCR Reagents (Applied Biosystems) and an ABI PRISM 7700 Sequence Detection System (Applied Biosystems).

Fluorescence-Activated Cell Sorting Analysis

The expression levels of P-gp on the cell surface after treatment with 10 μmol/L U0126 for 72 h were detected by fluorescence-activated cell sorting analysis using a human-specific monoclonal antibody, MRK16, raised against P-gp. Cells were incubated with or without a biotinylated $F(ab')_2$ fragment of MRK16 (100 μg/mL). The cells were then washed and incubated with R-phycoerythrin–conjugated streptavidin (400 μg/mL; Becton Dickinson and Company). Fluorescence staining levels were detected using FACSCalibur (Becton Dickinson and Company).

The cellular accumulation of rhodamine123, a substrate of P-gp, was determined by flow cytometry. Cells were treated with 10 μmol/L U0126 for 72 h, and the medium was changed every 24 h. After trypsinization, the cells (1×10^5) were washed with ice-cold PBS, resuspended in 1 mL of DMEM supplemented with 300 nmol/L rhodamine123, and incubated for 20 min at 37°C. The cells were then washed twice with ice-cold PBS, and the intracellular accumulation of rhodamine123 was measured using FACSCalibur.

Metabolic Labeling of P-gp in MDA-MB-231/3HisMDR Cells

To examine the biosynthesis profile of P-gp, MDA-MB-231/3HisMDR cells (1×10^6 cells/25 cm^2 flask) were incubated in methionine- and cysteine-free DMEM (Invitrogen) supplemented with 7% dialyzed charcoal/dextran-treated FBS (HyClone; labeling medium) for 1.5 h just before the beginning of the experiments. The cells were then incubated in the labeling medium containing 300 μCi/mL of [^{35}S]methionine/cysteine for either 0.5 or 1 h. For U0126-treated cells, 10 μmol/L U0126 was added at 4 h before the start of the experiment. Cells were then harvested and lysed with lysis buffer. 3HisP-gp was immunoprecipitated with Ni-NTA agarose and solubilized with 2× sample buffer as described above. The labeled protein was then subjected to SDS-PAGE and autoradiographed. The band intensities of the labeled P-gp were quantified using the NIH-Image densitometric program. Each column represents the mean ± SD from three independent experiments.

To examine the degradation of P-gp, MDA-MB-231/3HisMDR cells (1×10^6 cells/25 cm^2 flask) were incubated in the labeling medium for 1.5 h just before starting the experiment and then incubated in the labeling medium containing 300 μCi/mL of [^{35}S]methionine/cysteine for 1 h. The labeling medium was then replaced with the growth medium, and the cells were chased for 2 to 12 h. For U0126-treated cells, 10 μmol/L U0126 was added to the medium throughout the experiment. The band intensities of the labeled P-gp were again quantified using NIH Image and calculated as a percentage of the control (labeled sample with no chase; 0 h).

Results

The Inhibitors of MEK-ERK-RSK Pathway Suppress P-gp Expression

The human colorectal tumor cell lines HCT-15 and SW620-14, which both express endogenous P-gp, were treated with either 10 μmol/L FTI-277 (an inhibitor of farnesyltransferase that activates Ras), 10 μmol/L U0126 (a MEK1/2 inhibitor), 100 nmol/L 17-AAG (an inhibitor of heat shock protein 90 that stabilizes both Raf-1 and PDK1), 50 μmol/L LY294002 (a PI3K inhibitor), or 100 nmol/L rapamycin [an inhibitor of mammalian target of rapamycin (mTOR)] for 12 h. The P-gp expression levels were then determined by Western blot analysis. As shown in Fig. 1A, the cells treated with FTI-277, U0126, and 17-AAG showed 5- to 20-fold lower levels of P-gp compared with untreated cells. However, neither LY294002 nor rapamycin treatments affected P-gp expression. To exclude the possibility that the down-regulation of P-gp in these analyses was due to an alteration in the status and solubility of the protein in 0.2% NP40, we also analyzed its expression using whole cell lysates. In this experiment, U0126 and 17-AAG again suppressed P-gp expression in HCT-15 and SW620-14 cells (Fig. 1B). We next examined whether either SB203580 (a p38MAPK inhibitor) or SP600125 (a JNK inhibitor) affected P-gp expression levels in HCT-15 and SW620-14 cells. However, upon treatment with 10 μmol/L SB203580 or 20 μmol/L SP600125 for 12 h, the P-gp expression levels were found to be unchanged in these cells (Fig. 1C).

MEK Inhibitors Down-regulate P-gp Expression in a Time-Dependent Manner

We next examined the suppressive effects of U0126 in exogenous P-gp–expressing cells. We also examined the time dependency of the down-regulation of P-gp by U0126. HCT-15, SW620-14, MCF-7/MDR, and MDA-MB-231/MDR cells were treated with 10 μmol/L U0126 for 2 to 16 h, and P-gp expression levels were determined by Western blotting. U0126 was found to down-regulate exogenous P-gp expression also in these *MDR1*-transduced cell lines

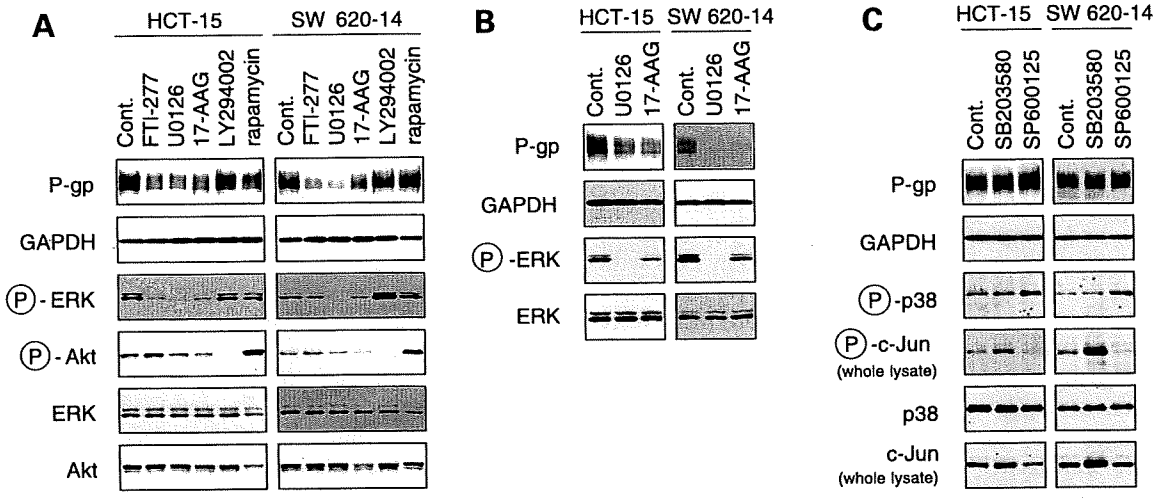

Figure 1. Screening of the effects of various kinase inhibitors upon P-gp expression levels. **A,** Western blot analysis of endogenous P-gp expression levels in both cell membrane and cytoplasmic fractions of cells treated with inhibitors against the MEK-ERK-RSK or PI3K-Akt-mTOR pathway. HCT-15 or SW620-14 cells were treated with either medium alone (*Cont.*), 10 μmol/L FTI-277, 10 μmol/L U0126, 100 nmol/L 17-AAG, 20 μmol/L LY294002, or 10 μmol/L rapamycin for 12 h. Cellular membrane and cytoplasmic fractions were prepared with lysis buffer containing 0.2% NP40 and subjected to Western blotting with the indicated antibodies. **B,** Western blot analysis of P-gp expression levels in whole-cell lysates of U0126- or 17-AAG – treated cells. HCT-15 or SW620-14 cells were treated with either medium alone, 10 μmol/L U0126, or 100 nmol/L 17-AAG. After 12 h, whole-cell lysates were obtained using lysis buffer containing 1% SDS and subjected to Western blotting with the indicated antibodies. **C,** Western blot analysis of P-gp expression levels in cells treated with p38MAPK or JNK inhibitor. HCT-15 or SW620-14 cells were treated with either medium alone, 10 μmol/L SB203580, or 20 μmol/L SP600125 for 12 h. Cells were harvested and divided into two groups. One was lysed with lysis buffer containing 1% SDS to analyze the expression levels of total c-Jun and phosphorylated c-Jun, and another was lysed with lysis buffer containing 0.2% NP40 to analyze the other indicated proteins. The lysates were then subjected to Western blotting with the indicated antibodies.

(Fig. 2A). The time dependency of this suppression varied among the cell lines, as it was evident within 4 h in SW620-14 cells, but required 8 h in HCT-15 and MCF-7/MDR cells and 12 h in MDA-MB-231/MDR cells. As a control experiment, we examined the time dependency of P-gp expression in the absence of the inhibitor. The same cells were cultured for a further 2 to 16 h after changing the medium to the flesh growth medium without inhibitors, and the P-gp levels were found to be unchanged at each time point for each cell line (Fig. 2B).

We next examined *MDR1* mRNA expression levels by RT-PCR. Each of the HCT-15, SW620-14, MCF-7/MDR, and MDA-MB-231/MDR cells were treated with U0126 under the same conditions used for the experiments in Fig. 2A. Total RNAs were isolated from these cells and RT-PCR was done using *MDR1* or *GAPDH*-specific oligonucleotides. As shown in Fig. 2C, the *MDR1* mRNA levels were unchanged after U0126 treatment at all time points in each of the cell lines. Similar results were obtained using real-time PCR analysis (Supplementary Fig. S1A).[3] P-gp expression levels were then examined in these cells after treatment with another MEK inhibitor, PD98059, at a concentration of 50 μmol/L for 8 or 12 h. Similar to the findings shown in Fig. 2A, all of the cell lines tested in this experiment expressed lower levels of P-gp after PD98059 treatment, compared with untreated cells (Fig. 2D).

We further examined the effects upon P-gp expression when either ERK or RSK was specifically suppressed by siRNA. Each of our four test cell lines was transfected with either a nonsilencing control, *ERK* siRNA, or *RSK* siRNA, and the P-gp expression levels were then determined by Western blotting after 48 h. P-gp was found to be down-regulated by the knockdown of both the ERK and RSK proteins in a dose-dependent manner (Fig. 2E). The suppression of RSK in particular had a significant negative effect upon P-gp expression (Fig. 2E). Fluorescence-activated cell sorting analysis also revealed that cells treated with U0126 for 72 h expressed lower amounts of cell surface P-gp compared with untreated cells (Fig. 3). From these data, we conclude that P-gp expression is suppressed by a blockade of the MEK-ERK-RSK pathway.

EGF or bFGF Stimulation Enhances P-gp Expression but Does Not Affect *MDR1* Transcription

Given that the inhibition of the MEK-ERK-RSK pathway suppressed P-gp expression, we next investigated whether the activation of this pathway would in fact enhance P-gp. HCT-15, SW620-14, MCF-7/MDR, and MDA-MB-231/MDR cells were cultured in serum-free DMEM for 6 h and incubated in the growth medium supplemented with 100 μg/L EGF for a further 2 to 16 h. Western blot analysis revealed that EGF activated EGFR (increased levels of phosphorylated EGFR are detectable), and that upon induction of the MEK-ERK-RSK pathway (increased phosphorylation of ERK) there was an observable increase in the P-gp expression levels in all cells (Fig. 4A). To examine the effects of serum starvation itself on P-gp

[3] Supplementary material for this article is available at Molecular Cancer Therapeutics Online (http://mct.aacrjournals.org/).

expression, the cells were cultured in serum-free DMEM for 6 h and then incubated in the growth medium only for a further 2 to 16 h. Phosphorylated ERK was found to have slightly increased in each of the four cell lines by the addition of FBS to the serum-starved culture, and this occurred simultaneously with increased P-gp expression levels (Fig. 4B). These data indicate that FBS itself activates the MEK-ERK-RSK pathway and increases P-gp expression. Moreover, the strong enhancement of P-gp expression by the stimulation of EGF and FBS persisted for a longer duration compared with the stimulation with FBS alone (Fig. 4A and B). However, although the P-gp levels were enhanced by EGF stimulation, the corresponding *MDR1* mRNA levels were unchanged, as indicated by our RT-PCR analysis (Fig. 4C; Supplementary Fig. S1B).[3] We next did bFGF treatments at 10 μg/L for 8 or 12 h using the same procedures described for Fig. 4A and a bFGF-dependent enhancement of P-gp expression was also observed in each cell line (Fig. 4D).

We next determined the effects upon P-gp expression levels by Western blotting when HCT-15 cells were transiently transfected with cDNAs corresponding to genes of either the MEK-ERK-RSK or PI3K-Akt signaling pathways. The activation of the MEK-ERK-RSK pathway by transfection with WT cDNAs for *H-Ras*, *Raf-1*, *MEK1*, *MEK2*, *ERK1*, *ERK2*, *RSK1*, or *RSK2* was found to enhance

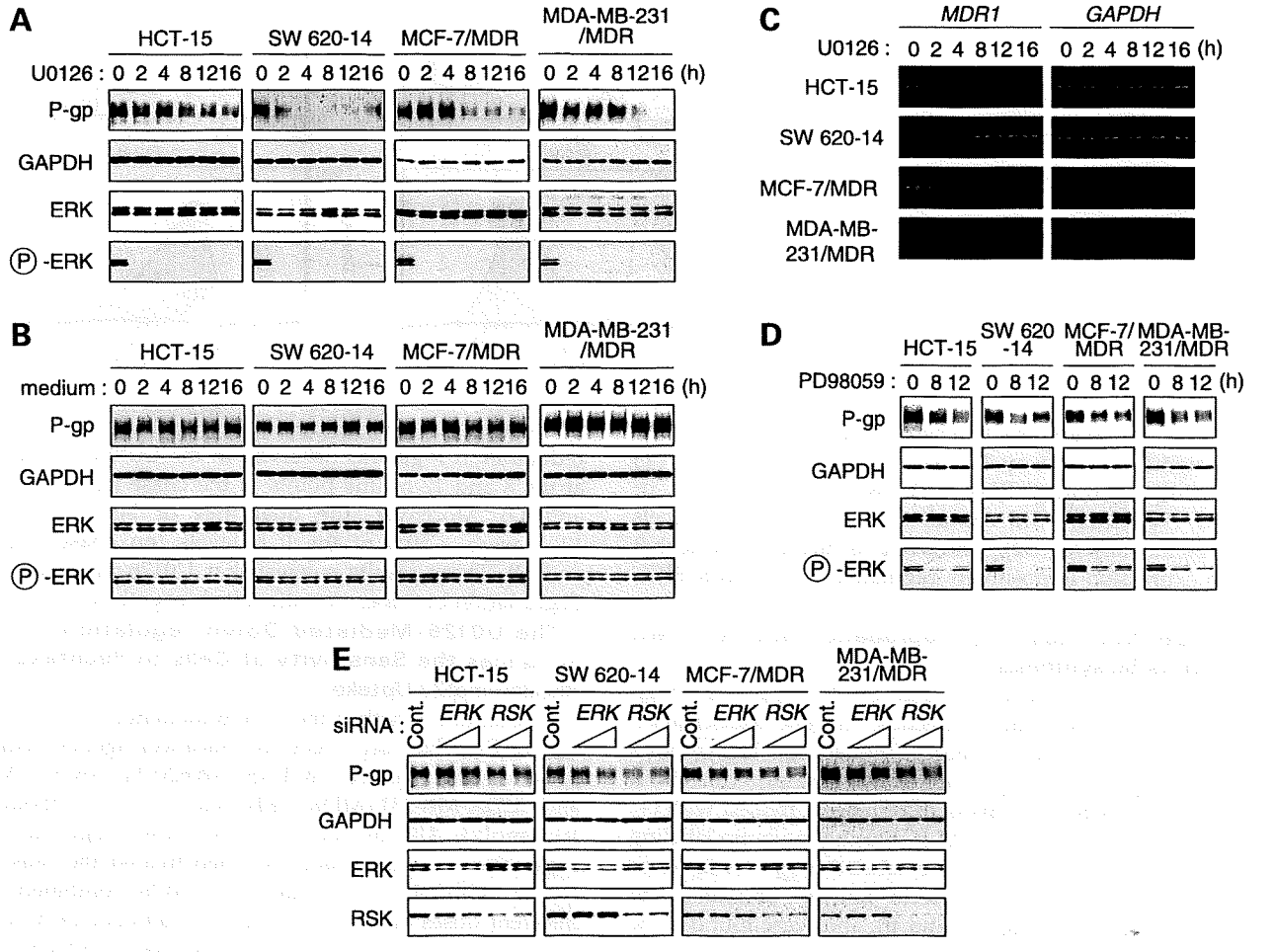

Figure 2. Down-regulation of P-gp by treatment with MEK inhibitors or by RNA interference of *MEK* and *ERK*. **A,** Western blot analysis of P-gp expression levels after a time course of U0126 treatment. HCT-15, SW620-14, MCF-7/MDR, or MDA-MB-231/MDR cells were treated with medium alone or with 10 μmol/L U0126 for 2 to 16 h. Cellular membrane and cytoplasmic fractions were prepared using lysis buffer containing 0.2% NP40 and subjected to Western blotting with the indicated antibodies. **B,** Western blot analysis of P-gp expression levels after a time course of treatment with medium alone. HCT-15, SW620-14, MCF-7/MDR, or MDA-MB-231/MDR cells were treated with medium alone for 2 to 16 h and processed as described in **A. C,** RT-PCR analysis of *MDR1* mRNA levels over a time course of U0126 treatment. After treatment with medium alone or with 10 μmol/L U0126 for 2 to 16 h in HCT-15, SW620-14, MCF-7/MDR, or MDA-MB-231/MDR cells, total RNAs were extracted from the cells. The mRNA levels of the *MDR1* and *GAPDH* genes were analyzed by RT-PCR as described in Materials and Methods. **D,** P-gp expression levels in PD98059-treated HCT-15, SW620-14, MCF-7/MDR, or MDA-MB-231/MDR cells. The cells were treated with medium alone or with 50 μmol/L PD98059 for 8 or 12 h and processed as described in **A. E,** the effects of *ERK* and *RSK* siRNAs on P-gp expression levels. HCT-15, SW620-14, MCF-7/MDR, or MDA-MB-231/MDR cells were transfected with siRNAs in the following combinations: 50 μmol/L negative control siRNA (*Cont.*); 25 or 50 μmol/L (each 12.5 or 25 μmol/L) of an *ERK1+ERK2* siRNA combination; or 25 or 50 μmol/L (each 8.3 or 16.7 μmol/L) of an *RSK1/RSK2/RSK3* siRNA mixture. After transfection for 48 h, the cells were harvested and lysed with lysis buffer containing 0.2% NP40. Cell lysates were then subjected to Western blotting with the indicated antibodies.

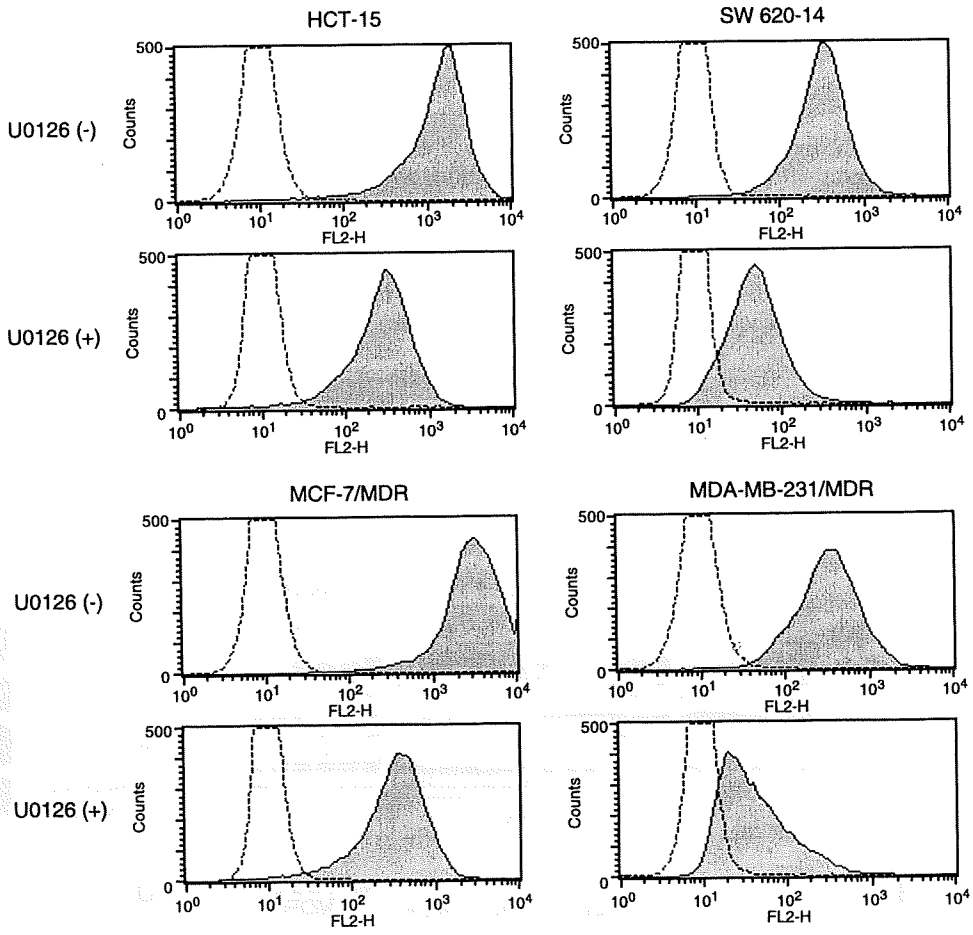

Figure 3. The down-regulation of cell surface P-gp expression by U0126. HCT-15, SW620-14, MCF-7/MDR, or MDA-MB-231/MDR cells were treated with medium alone or with 10 μmol/L U0126 for 72 h, with medium replacement every 24 h. The cells were then harvested with trypsin, washed with PBS, and incubated with (*closed areas*) or without (*open areas*) a biotinylated $F(ab')_2$ fragment of the MRK16 antibody. The cells were then washed with PBS and incubated with R-phycoerythrin–conjugated streptavidin. Fluorescence staining was then evaluated using FACSCalibur.

the P-gp expression levels, whereas the activation of PI3K-Akt signaling pathway by transfection with *p85α* (WT) regulatory subunit of *PI3K*, *akt1* (WT), *PTEN* (C124S), or *PTEN* (WT) DNA did not affect P-gp expression levels (Supplementary Fig. S2).[3] These results further indicate that P-gp expression is positively regulated by the MEK-ERK-RSK pathway.

U0126 Promotes P-gp Degradation but Does Not Inhibit Its Biosynthesis

Based on our observation that U0126 suppresses P-gp expression levels without affecting its gene transcription (Fig. 2A and C), we further examined the biosynthesis and degradation of P-gp using pulse-chase experiments in which MDA-MB-231/3HisMDR cells were treated with (+) or without (−) 10 μmol/L U0126. During the pulse labeling procedure for 0.5 or 1 h, the labeled P-gp levels were observed to gradually increase in both the untreated and U0126-treated cells (Fig. 5A and B), and were found to be almost equivalent in both cases. To subsequently examine the effects of U0126 on P-gp degradation, ^{35}S metabolic labeling was done for 1 h using MDA-MB-231/3HisMDR cells in the absence (−) or presence (+) of 10 μmol/L U0126. The cells were then chased for 2 to 12 h in the growth medium without (−) or with (+) 10 μmol/L U0126. The labeled P-gp expression levels were found to be largely unchanged in the untreated cells, but a significant reduction in P-gp was observed in the U0126-treated cells at the 8 and 12 h time points of the chase period (Fig. 5C and D). Moreover, the quantities of labeled P-gp at 12 h were ~50% of the 0 h levels (no chase; Fig. 5C and D). These results suggest that U0126 promotes P-gp degradation but does not affect its biosynthesis.

The U0126-Mediated Down-regulation of P-gp Enhances the Sensitivity of Cells to Paclitaxel and Rhodamine123 Uptake

To examine whether the U0126-mediated down-regulation of P-gp has any effect on anticancer agent–mediated apoptosis, we treated HCT-15, SW620-14, MCF-7/MDR, and MDA-MB-231/MDR cells with (+) or without (−) 10 μmol/L U0126 for 72 h to down-regulate P-gp expression on cell surface. We then treated the cells with (+) or without (−) 10 μmol/L U0126 combined with different doses of paclitaxel for an additional 24 h. In this experiment, the IC_{50} values (the dosage at which a 50% inhibition of cell growth occurs) for paclitaxel had been previously determined for each cell line, and the cells were treated with both this dose and a 3-fold higher concentration of the drug. As shown in Fig. 6A, paclitaxel increased the levels of cleaved PARP, which is a substrate of caspase-3, as reported previously (17). When the cells were

pretreated with U0126, the extent of this PARP cleavage by paclitaxel was enhanced in each cell lines, particularly at the 3-fold IC_{50} concentrations (Fig. 6A). These results indicate that paclitaxel-mediated apoptosis signaling via the activation of caspase-3 is enhanced by the U0126-mediated suppression of P-gp.

Finally, we examined the effects of U0126 on rhodamine123 uptake in P-gp–expressing cells. As shown in Fig. 6B, cells treated with U0126 accumulated higher levels of rhodamine123 compared with untreated cells. Hence, the U0126-mediated down-regulation of P-gp leads to an increase in the intracellular concentration of P-gp substrates.

Discussion

Many previous studies have evaluated P-gp inhibitors to effectively reverse P-gp–mediated drug resistance. In the 1980s, verapamil was initially identified as a P-gp inhibitor (18, 19), as it increases the intracellular concentration of various anticancer agents in multidrug-resistant cells by binding P-gp and inhibiting drug efflux. Subsequently, many P-gp inhibitors such as valspoder (PSC-833), dofequidar fumarate (MS-209), tariquidar (XR9576), and thiosemicarbazone derivative (NSC73306), have been developed (20–23). Clinical trials using such P-gp inhibitors have shown *in vivo* increases in the intracellular concentrations of coadministered anticancer agents in P-gp–positive tumor cells (24). However, phase III trials of these agents have not been successful, and no significant survival benefit as a result of P-gp inhibition has yet been achieved (25, 26). Further clinical studies using new P-gp inhibitors and new combination-treatment regimens have been devised, and some are currently ongoing.

The regulatory mechanisms underlying the expression of ABC transporters, including P-gp and BCRP, have not yet been well clarified. We have previously shown that physiologic levels of estrogens suppress P-gp and BCRP in estrogen receptor α–expressing breast cancer cells via posttranscriptional processes, and that this occurs without any affects upon transcription (14, 15). Other groups have also shown that the stability of P-gp is regulated by the ubiquitin-proteasome system (27, 28). Furthermore, Akt signaling has been shown to modulate a side population cell phenotype by regulating the expression of Bcrp1 in mouse (29). The PI3K inhibitor, LY294002, and a dominant-negative form of Akt have also been reported to down-regulate BCRP expression levels (16). Thus, the association between the expression of ABC transporter proteins and either cell growth signaling or the ubiquitin-proteasome system has recently generated some interest. In our present

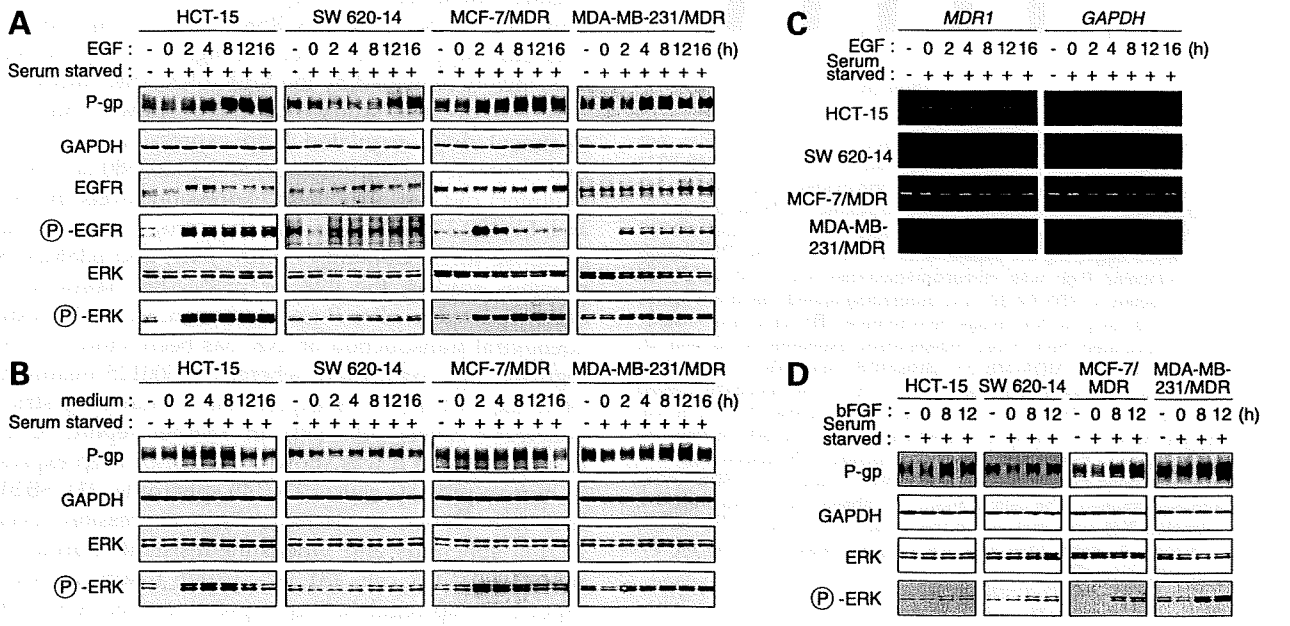

Figure 4. The up-regulation of P-gp by EGF or bFGF in a time-dependent manner. **A,** Western blot analysis of P-gp expression levels after the EGF-dependent activation of the MEK-ERK-RSK pathway. HCT-15, SW620-14, MCF-7/MDR, or MDA-MB-231/MDR cells were cultured in medium without serum for 6 h (*Serum starved*; +). The medium was then replaced with the growth medium supplemented with 100 μg/L EGF, and the cells were incubated for a further 2 to 16 h. Negative control cells were not serum starved and were untreated (*Serum starved*; – and *EGF*; –). Cellular membrane and cytoplasmic fractions were lysed with lysis buffer containing 0.2% NP40 and subjected to Western blotting with the indicated antibodies. **B,** Western blot analysis of P-gp expression levels after FBS-dependent activation of the MEK-ERK-RSK pathway. HCT-15, SW620-14, MCF-7/MDR, or MDA-MB-231/MDR cells were cultured in medium without serum for 6 h (*Serum starved*; +). The medium was then replaced with the flesh growth medium, and the cells were incubated for a further 2 to 16 h. Negative control cells and cell processing were as described in **A. C,** RT-PCR analysis of *MDR1* mRNA levels after EGF treatment. After treatment with EGF as in **A,** total RNAs were extracted from the cells and the mRNA levels of the *MDR1* and *GAPDH* genes were analyzed by RT-PCR. **D,** Western blot analysis of P-gp expression levels after bFGF treatment. HCT-15, SW620-14, MCF-7/MDR, or MDA-MB-231/MDR cells were cultured in medium without serum (*Serum starved*; +) and after incubation for 6 h, the medium was replaced with the growth medium supplemented with 10 μg/L bFGF, and the cells were cultured for a further 8 or 12 h. Negative control cells and cell processing were as described in **A.**

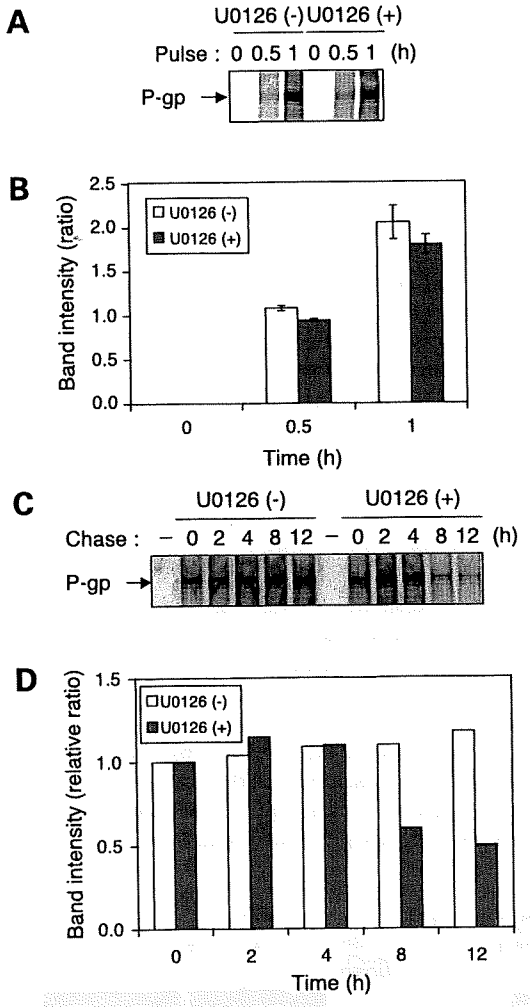

Figure 5. U0126 promotes the degradation of P-gp but does not suppress its biosynthesis. **A** and **B**, biosynthesis of P-gp. MDA-MB-231/3HisMDR cells were cultured in methionine- and cysteine-free medium for 1.5 h and then metabolically labeled with 300 μCi/mL of ^{35}S for 0.5 or 1 h. For the U0126 treatment, the cells were treated with 10 μmol/L U0126 from 4 h before beginning the experiments to the end of the ^{35}S-labeling period. ^{35}S-labeled P-gp was immunoprecipitated from 500 μg of cell lysates, subjected to SDS-PAGE, and autoradiographed. Band intensities were measured using an NIH Image densitometer (**B**). *Columns*, means; *bars*, SD; calculated from three independent experiments. **C** and **D**, degradation of P-gp. MDA-MB-231/3HisMDR cells were cultured in methionine- and cysteine-free medium for 1.5 h, metabolically labeled with 300 μCi/mL of ^{35}S for 1 h, and chased for a further 2 to 12 h. For U0126 treatment, the cells were treated with 10 μmol/L U0126 from the time of ^{35}S labeling to the end of the chase period. ^{35}S-labeled P-gp was immunoprecipitated from 500 μg of cell lysates, subjected to SDS-PAGE, and autoradiographed. The cells without ^{35}S labeling were also prepared, and unlabeled P-gp was analyzed in the same manner as the ^{35}S-labeled P-gp (*Chase*; –). Band intensities were again measured using an NIH Image densitometer (**D**).

study, we have attempted to further clarify the regulatory mechanisms underlying ABC transporter protein expression, focusing on P-gp, to identify inhibitors that specifically target these expression mechanism(s).

We initially found that inhibitors of the MEK-ERK-RSK pathway suppressed P-gp expression (Fig. 1). In particular, the MEK inhibitor U0126 was found to potently down-regulate endogenous P-gp expression (Fig. 1), and both the U0126- and PD98059-mediated down-regulation of P-gp could be observed in both endogenous and exogenous P-gp–expressing cells (Fig. 2A and D). Moreover, these phenomena were found not to be the result of transcriptional regulation (Fig. 2C; Supplementary Fig. S1A).[3] The suppression of P-gp by MEK inhibitors was also far more rapid compared with estrogens (Fig. 2A and D, compared with ref. 15). ERK and RSK knockdown by siRNAs also down-regulated P-gp expression (Fig. 2E). Conversely, the activation of the MEK-ERK-RSK pathway by the overexpression of WT proteins for H-Ras, Raf-1, MEK1, MEK2, ERK1, ERK2, RSK1, or RSK2 enhanced P-gp expression in HCT-15 cells, whereas the activation of the PI3K-Akt signaling pathway by overexpressing the phosphatase inactive form of PTEN (C124S), p85α (WT) regulatory subunit of PI3K, or Akt (WT) did not affect P-gp in these cells (Supplementary Fig. S2).[3] These results suggest that the stability of P-gp is regulated by the MEK-ERK-RSK pathway, and that the kinase activities of RSK are necessary for this stabilization. Although BCRP has been shown to be regulated by the PI3K-Akt signaling pathway (16), it is likely that P-gp is regulated by different mechanisms. We additionally examined P-gp expression in cells treated with EGF and bFGF, which are activators of the MEK-ERK-RSK pathway via EGFR and FGF receptor, respectively. As expected, the stimulation of either EGF or bFGF enhanced P-gp expression levels without affecting its transcription (Fig. 4A–D; Supplementary Fig. S1B).[3] Moreover, the presence of FBS in the growth medium slightly enhanced the P-gp expression levels with the activation of the MEK-ERK-RSK pathway (Fig. 4B). These data thus support our earlier findings that P-gp expression is positively regulated by the MEK-ERK-RSK pathway.

In the present study, we have shown that U0126 treatment down-regulated P-gp expression for 12 h, but that SP600125 (a JNK inhibitor) and SB203580 (a p38MAPK inhibitor) did not alter these expression levels in HCT-15 and SW620-14 cells (Fig. 1). The components of MAPK comprise three subfamilies, ERK, JNK, and p38MAPK. In previous studies, the JNK or p38MAPK pathways have been reported to alter P-gp expression levels. In addition, adenoviral transduction of *JNK* has been shown to down-regulate P-gp expression, whereas SP600125 treatment for 24 h did not affect its expression in human gastric and pancreatic cancer cells (30). In another report, SP600125 treatment for 24 h was shown to enhance P-gp expression in human prostate cancer DU145 spheroids (31). SB203580 has been shown to decrease P-gp expression levels in DU145 spheroids and vincristine-resistant murine leukemia L1210/VCR cells (31, 32). U0126 treatment was also reported to up-regulate P-gp expression after 24 h in DU145 spheroids (31). The discrepancies between the data from these previous reports and our present experiments may be due to differences in the cell lines and treatment protocols used. We observed that the down-regulation of phosphorylated ERK by U0126 was slightly recovered at 24 h in each of the cell lines tested in this study (data not shown),

suggesting that U0126 may be degraded. Therefore, we replenished the U0126-containing medium every 24 h in the experiments shown in Figs. 3 and 6.

Although U0126 suppressed both endogenous and exogenous P-gp, the *MDR1* mRNA levels were unaffected by treatment with this agent (Fig. 2C; Supplementary Fig. S1A).[3] These data strongly indicate the existence of U0126-mediated posttranscriptional P-gp regulation mechanism(s), most likely to be translation and degradation processes. To further elucidate this, we established MDA-MB-231/3HisMDR cells and found that the rate of P-gp biosynthesis in U0126-treated cells was virtually equivalent to the untreated cells (Fig. 5A and B). In contrast, however, the degradation rate of P-gp in U0126-treated cells was higher than in untreated cells (Fig. 5C and D). We subsequently did a pulse-chase experiment to confirm these observations and found that the P-gp expression levels in untreated cells were constant up to the 12 h time point,

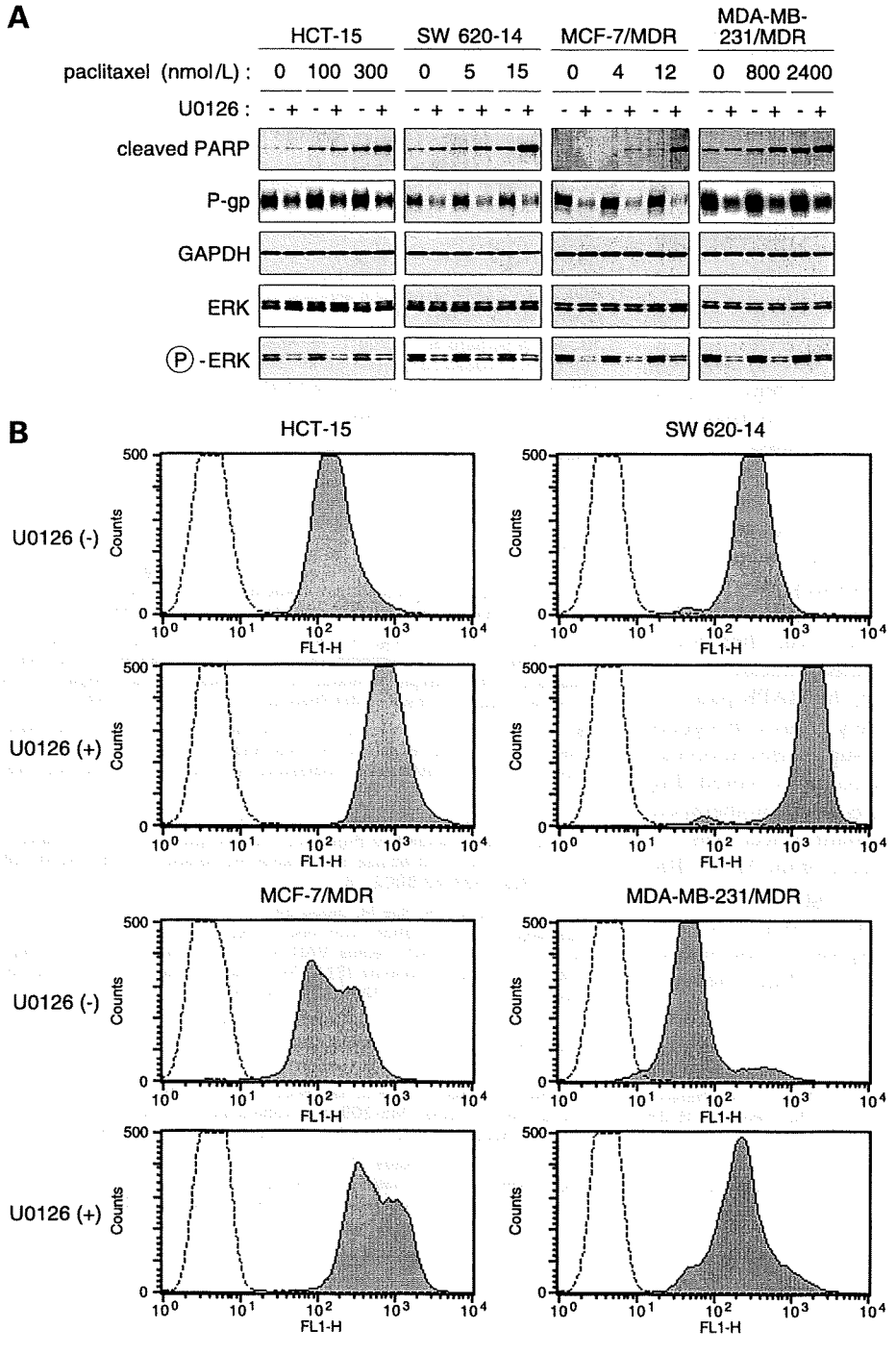

Figure 6. The physiologic effects of U0126 upon the function of P-gp as an efflux pump. **A,** Western blot analysis of cleaved PARP after paclitaxel treatment combined with U0126. HCT-15, SW620-14, MCF-7/MDR, or MDA-MB-231/MDR cells were treated with medium alone (*U0126*; –) or with 10 μmol/L U0126 (*U0126*; +) for 72 h, with medium replacement every 24 h. The cells were then further treated with or without 10 μmol/L U0126 and/or paclitaxel as the indicated combinations for 24 h. Paclitaxel was used at both 1× and 3× its predetermined IC_{50} concentration for each cell line. The cells were harvested with lysis buffer containing 0.2% NP40 and the cell lysates were subjected to Western blotting with the indicated antibodies. **B,** fluorescence-activated cell sorting analysis of rhodamine123 uptake in U0126-treated cells. HCT-15, SW620-14, MCF-7/MDR, or MDA-MB-231/MDR cells were treated with medium alone [*U0126 (–)*] or with 10 μmol/L U0126 [*U0126 (+)*] for 72 h, with medium replacement every 24 h. The cells were then trypsinized and adjusted to a concentration of 5×10^5/mL with medium. The cells were incubated with 300 nmol/L rhodamine123 for 20 min at 37°C and washed twice with ice-cold PBS. The intracellular accumulation of rhodamine123 was detected using FACSCalibur.

but that the levels in the U0126-treated cells had decreased by ~50% during the same 8 to 12 h chase period (Fig. 5C and D). These results indicate that U0126 suppresses P-gp expression by promoting its degradation.

To analyze the physiologic responses to the U0126-mediated down-regulation of P-gp, we examined the possible effects of this response upon the enhancement of apoptosis by paclitaxel, and also upon the accumulation of rhodamine123, both of which are substrates of P-gp (33). Because PARP is cleaved by active caspase-3, an apoptosis inducer (17, 34), we used this as the index of the paclitaxel-mediated enhancement of apoptosis signaling. P-gp expression on the cell surface decreased when the cells were treated with U0126 for 72 h (Fig. 3). The cells in this experiment were therefore pretreated with U0126 for 72 h and then cotreated with U0126 and paclitaxel for a further 24 h. The combination of U0126 and paclitaxel was found to enhance the levels of cleaved PARP, compared with paclitaxel exposure alone (Fig. 6A). In addition, the intracellular rhodamine123 levels were also found to accumulate after U0126 treatment for 72 h (Fig. 6B). These results indicate that the U0126-mediated down-regulation of P-gp can reverse the P-gp–mediated resistance to anticancer agents.

Although we show that inhibition of the MEK-ERK-RSK pathway suppresses P-gp expression, and that this involves the kinase activities of RSKs (Fig. 2E; Supplementary Fig. S2A),[3] it remains unclear how MEK inhibitors promote P-gp degradation or whether the RSKs directly regulate P-gp expression. If these molecules indirectly regulate P-gp degradation, the question of which factors are associated with this mechanism remains to be elucidated and will require further molecular analyses.

Many P-gp inhibitors that have been developed are competitors of anticancer agents that are also P-gp substrates. Because RSKs have been shown to positively regulate P-gp expression in our present study, we speculate that MEK, ERK, and RSK inhibitors, and also RNA interferences may have potential as novel therapeutic agents for the reversal of P-gp–mediated anticancer drug resistance. During cellular hyperplasia, the MAPK pathway is often activated and provides a variety of growth signals, promotes cell cycle progression, and suppresses apoptosis (9). Inhibitors of the MEK-ERK-RSK pathway would thus be expected to have significant benefits as chemotherapeutics against P-gp–mediated drug-resistant cancer cells.

In conclusion, we show that a blockade of the MEK-ERK-RSK pathway suppresses cell surface P-gp expression by promoting its degradation. Our data therefore provide new insights into the regulation of P-gp expression and suggest potential new strategies for the reversal of P-gp–mediated anticancer drug resistance.

References

1. Gottesman MM, Hrycyna CA, Schoenlein PV, Germann UA, Pastan I. Genetic analysis of the multidrug transporters. Annu Rev Genet 1995;29:607–49.

2. Riordan JR, Deuchars K, Kartner N, Alon N, Trent J, Ling V. Amplification of P-glycoprotein genes in multidrug-resistant mammalian cell lines. Nature 1985;316:817–9.

3. Chen CJ, Chin JE, Ueda K, et al. Internal duplication and homology with bacterial transport proteins in the *mdr*1 (P-glycoprotein) gene from multidrug-resistant human cells. Cell 1986;47:381–9.

4. Shen DW, Fojo A, Chin JE, et al. Human multidrug-resistant cell lines: increased *mdr1* expression can precede gene amplification. Science 1986;232:643–5.

5. Gupta S, Gollapudi. P-glycoprotein (MDR-1 gene product) in cells of the immune system: its possible physiologic role and alteration in ageing and human immunodeficiency virus-1 (HIV-1) in function. J Clin Invest 1993;13:289–301.

6. Ludescher C, Pall G, Irschick EU, Gasti G. Differential activity of P-glycoprotein in normal blood lymphocyte subset. Br J Haematol 1998;101:722–7.

7. Puddu P, Fais S, Luciani F, et al. Interferon-γ up-regulates expression and activity of P-glycoprotein in human peripheral blood monocyte-derived macrophages. Lab Invest 1999;79:1299–309.

8. Goldstein LJ, Galski H, Fojo A, et al. Expression of a multidrug resistance gene in human cancers. J Natl Cancer Inst 1989;81:116–24.

9. Chang F, Steelman LS, Lee JT, et al. Signal transduction mediated by the Ras/Raf/MEK/ERK pathway from cytokine receptors to transcription factors: potential targeting for therapeutic intervention. Leukemia 2003;17:1263–93.

10. Traverse S, Cohen P, Paterson H, Marshall, C, Rapp U, Grand JA. Specific association of activated MAP kinase kinase kinase (Raf) with the plasma-membranes of Ras-transformed retinal cells. Oncogene 1993;8:3175–81.

11. Djaborkhel R, Tvrdík D, Eckschlager T, Raska I, Müller J. Cyclin A down-regulation in TGFβ1-arrested follicular lymphoma cells. Exp Cell Res 2000;261:250–9.

12. Nagata D, Suzuki E, Nishimatsu H, et al. Transcriptional activation of the cyclin D_1 gene is mediated by multiple *cis*-elements. including SP1 sites and a cAMP-responsive element in vascular endothelial cells. J Biol Chem 2001;276:662–9.

13. Fujita S, Sato S, Tsuruo T. Phosphorylation of $p27^{Kip1}$ at threonine 198 by p90 ribosomal protein S6 kinases promotes its binding to 14-3-3 and cytoplasmic localization. J Biol Chem 2003;278:49254–60.

14. Imai Y, Ishikawa E, Asada S, Sugimoto Y. Estrogen-mediated post transcriptional down-regulation of breast cancer resistance protein/ABCG2. Cancer Res 2005;65:596–604.

15. Mutoh K, Tsukahara S, Mitsuhashi J, Katayama K, Sugimoto Y. Estrogen-mediated post transcriptional down-regulation of P-glycoprotein in MDR1-transduced human breast cancer cells. Cancer Sci 2006;97:1198–204.

16. Takada T, Suzuki H, Gotoh Y, Sugiyama Y. Regulation of the cell surface expression of human BCRP/ABCG2 by the phosphorylation state of Akt in polarized cells. Drug Metab Dispos 2005;33:905–9.

17. Chunrong YU, Wang S, Dent P, Grant S. Sequence-dependent potentiation of paclitaxel-mediated apoptosis in human leukemia cells by inhibitors of the mitogen-activated protein kinase kinase/mitogen-activated protein kinase pathway. Mol Pharmacol 2001;60:143–54.

18. Tsuruo T, Iida H, Tsukagoshi S, Sakurai Y. Overcoming of vincristine resistance in P388 leukemia *in vivo* and *in vitro* through enhanced cytotoxicity of vincristine and vinblastine by verapamil. Cancer Res 1981;41:1967–72.

19. Yusa K, Tsuruo T. Reversal mechanism of multidrug resistance by verapamil: direct binding of P-glycoprotein on specific sites and transport of verapamil outward across the plasma membrane of K562/ADM cells. Cancer Res 1989;49:5002–6.

20. Friedenberg WR, Rue M, Blood EA, et al. Phase III study of PSC-833 (valspodar) in combination with vincristine, doxorubicin, and dexamethasone (valspodar/VAD) versus VAD alone in patients with recurring or refractory multiple myeloma (E1A95): a trial of the Eastern Cooperative Oncology Group. Cancer 2006;106:830–8.

21. Saeki T, Tsuruo T, Sato W, Nishikawa K. Drug resistance in chemotherapy for breast cancer. Cancer Chemother Pharmacol 2005;56:s84–9.

22. Dieras V, Bonneterre J, Laurence V, et al. Phase I combining a P-glycoprotein inhibitor, MS-209, in combination with docetaxel in patients with advanced malignancies. Clin Cancer Res 2005;11:6256–60.

23. Ludwig JP, Szakács G, Martin SE, et al. Selective toxicity of NSC73306 in MDR1-positive cells as a new strategy to circumvent multidrug resistance in cancer. Cancer Res 2006;66:4808–15.

24. Tidefelt U, Liliemark J, Gruber A, et al. P-glycoprotein inhibitor valspodar (PSC 833) increases the intracellular concentrations of daunorubicin *in vivo* in patients with P-glycoprotein-positive acute myeloid leukemia. J Clin Oncol 2000;18:1837 – 44.

25. Nicolantonio FD, Knight LA, Glaysher S, et al. *Ex vivo* reversal of chemoresistance by tariquidar (XR9576). Anticancer Drugs 2004;15:861 – 9.

26. Robert J, Jarry C. Multidrug resistance reversal agents. J Med Chem 2003;46:4805 – 17.

27. Zhang Z, Wu JY, Hait WN, Yang JM. Regulation of the stability of P-glycoprotein by ubiquitination. Mol Pharmacol 2004;66:395 – 403.

28. Loo TW, Clarke DM. The human multidrug resistance P-glycoprotein is inactive when its maturation is inhibited: potential for a role in cancer chemotherapy. FASEB J 1999;13:1724 – 32.

29. Mogi M, Yang J, Lambert JF, et al. Akt signaling regulates side population cell phenotype via Bcrp1 translocation. J Biol Chem 2003;278: 39068 – 75.

30. Zhou J, Liu M, Aneja R, Chandra R, Lage H, Joshi HC. Reversal of P-glycoprotein-mediated multidrug resistance in cancer cells by the c-Jun NH_2-teriminal kinase. Cancer Res 2006;66:445 – 51.

31. Wartenberg M, Gronczynska S, Bekhite MM, et al. Regulation of the multidrug resistance transporter P-glycoprotein in multicellular prostate tumor spheroids by hyperthermia and reactive oxygen species. Int J Cancer 2005;113:229 – 40.

32. Barancik M, Bohacova V, Kvackajova J, Hudecova S, Krizanova O, Breier A. SB203580, a specific inhibitor of p38-MAPK pathway, is a new reversal agent of P-glycoprotein-mediated multidrug resistance. Eur J Pharm Sci 2001;14:29 – 36.

33. Hegewisch-Becker S, Hanania EG, Fu S, Korbling M, Deisseroth AB, Andreeff M. Transduction of MDR1 into human and mouse haemopoietic progenitor cells: use of rhodamine (Rh123) to determine transduction frequency and *in vivo* selection. Br J Haematol 1995;90:876 – 83.

34. He J, Whitacre CM, Xue LY, Berger NA, Oleinick NL. Protease activation and cleavage of poly(ADP-ribose) polymerase: an integral part of apoptosis in response to photodynamic treatment. Cancer Res 1998;58: 940 – 6.

Pharmaceutical Research, Vol. 24, No. 6, June 2007 (© 2007)
DOI: 10.1007/s11095-007-9235-2

Research Paper

The Identification of Two Germ-line Mutations in the *Human Breast Cancer Resistance Protein* Gene that Result in the Expression of a Low/Non-functional Protein

Sho Yoshioka,[1] Kazuhiro Katayama,[1] Chikako Okawa,[1] Sachiko Takahashi,[1] Satomi Tsukahara,[2] Junko Mitsuhashi,[1,2] and Yoshikazu Sugimoto[1,2,3]

Received September 11, 2006; accepted January 2, 2007; published online March 21, 2007

Purpose. We examined the effects of the nine nonsynonymous germ-line mutations/SNPs in the *breast cancer resistance protein (BCRP/ABCG2)* gene on the expression and function of the protein.
Materials and Methods. We generated cDNAs for each of these mutants (G151T, C458T, C496G, A616C, T623C, T742C, T1291C, A1768T, and G1858A *BCRP*) and compared the effects of their exogenous expression in PA317 cells with a wild-type control.
Results. PA/F208S cells (T623C *BCRP*-transfectants) expressed marginal levels of a BCRP protein species (65 kDa), which is slightly smaller than wild-type (70 kDa), but this mutant did not appear on the cell surface or confer drug resistance. PA/F431L cells (T1291C *BCRP*-transfectants) were found to express both 70 kDa and 65 kDa BCRP protein products. In addition, although PA/F431L cells expressed 70 kDa BCRP at comparable levels to PA/WT cells, they showed only marginal resistance to SN-38. PA/T153M cells (C458T *BCRP*-transfectants) and PA/D620N cells (G1858A *BCRP*-transfectants) expressed lower amounts of BCRP and showed lower levels of resistance to SN-38 compared with PA/WT cells.
Conclusions. We have shown that T623C *BCRP* encodes a non-functional BCRP and that T1291C *BCRP* encodes a low-functional BCRP. Hence, these mutations may affect the pharmacokinetics of BCRP substrates in patients harboring these alleles.

KEY WORDS: BCRP/ABCG2; drug resistance; SN-38; SNPs.

INTRODUCTION

ATP binding cassette (ABC) transporters, such as P-glycoprotein (P-gp) and MRP1, are responsible for the acquisition of multidrug resistance in cancer cells (1–3). These transporters pump out various structurally unrelated anticancer drugs in an ATP-dependent manner. Breast cancer resistance protein (BCRP/ABCG2) is a half-molecule ABC transporter harboring an N-terminal ATP binding domain and a C-terminal transmembrane domain that mediates resistance to SN-38 (an active metabolite of irinotecan), mitoxantron, and topotecan (4–8). We previously reported that BCRP forms a homodimer via Cys-603 interactions and that these homodimeric complexes function as an efflux pump for anticancer agents (9,10). We have also reported earlier that BCRP exports sulfated estrogens, suggesting that there is a physiological role of BCRP for the tissue distribution and excretion of steroid hormones (11). BCRP is also widely expressed in normal human tissues such as the placenta, intestine, kidney, liver, prostate, ovary, testis, and hematopoietic stem cells (5,12,13). BCRP is assumed to play a role in the protective functions of the maternal-placental barrier, blood-testis barrier and hematopoietic stem cells against toxic substances and metabolites (14,15). BCRP has also shown to be expressed in the mammary gland during lactation and, it seems to be responsible for the active secretion of the BCRP substrates into milk (16).

In our previous study, we identified three nonsynonymous SNPs within the *BCRP* gene, G34A substituting Met for Val-12 (V12M), C376T substituting a stop codon for Gln-126 (Q126Stop), and C421A substituting Lys for Gln-141 (Q141K). G34A *BCRP* cDNA-transfected cells were found to express similar amounts of BCRP protein and further showed similar levels of SN-38 resistance compared with wild-type *BCRP* cDNA-transfected cells. In contrast C376T *BCRP* cDNA encodes a nonfunctional protein and C421A *BCRP* cDNA-transfected cells expressed a lower amount of BCRP protein and showed lower resistance to SN-38 than wild-type *BCRP* transfected cells (17). More-

[1] Department of Chemotherapy, Kyoritsu University of Pharmacy, 1-5-30 Shibakoen, Minato-ku, Tokyo, 105-8512, Japan.
[2] Division of Gene Therapy, Cancer Chemotherapy Center, Japanese Foundation for Cancer Research, Tokyo, Japan.
[3] To whom correspondence should be addressed. (e-mail: sugimoto-ys@kyoritsu-ph.ac.jp)

ABBREVIATIONS: ABC transporter, ATP-binding cassette transmembrane transporter; BCRP, breast cancer resistance protein; DHFR, dihydrofolate reductase; GAPDH, glyceraldehyde-3-phosphate dehydrogenase; IRES, internal ribosome entry site; SNPs, single nucleotide polymorphisms.

Table I. Frequencies of Germ-line Mutations/SNPs Within The *BCRP* Gene

Variation		Frequency (%)	Number	Population	Reference
Nucleotide	Amino acid				
G34A	V12M	19	29	Japanese	17
G151T	G51C	0.1[a]	350	Japanese	
C376T	Q126Stop	1.2	124	Japanese	17
C421A	Q141K	26.6	124	Japanese	17
C458T	T153M	3.3	30	Cell line	32
C496G	Q166E	0.3[a]	200	Japanese	
A616C	I206L	20	10	Hispanic	33
T623C	F208S	0.3[a]	200	Japanese	
T742C	S248P	0.5[a]	200	Japanese	
T1291C	F431L	0.6[b]	260	Japanese	34
A1768T	N590Y	1.1	88	Caucasians	33
G1858A	D620N	1.1	90	unknown	35

[a] Determined in this study.
[b] Determined in this study and in previous reports (frequencies and patient numbers are combined).

over, as C421A *BCRP* expresses low levels of protein, it was reported to affect the pharmacokinetics of patients harboring this allele who had been treated with an intracavernous administration of difromotecan (18). C421A *BCRP* was also reported to affect the pharmacokinetics of rosuvastain in healthy Chinese males (19).

In our present study, we generated nine *BCRP* cDNAs, each carrying a nonsynonymous germ-line mutation/SNP that has been already published or reported in a database. The effects of these different mutations on BCRP expression and function were examined in cells exogenously expressing these cDNAs.

MATERIALS AND METHODS

BCRP Expression Vectors

We generated nine cDNAs corresponding to the *BCRP* germ-line mutations/SNPs, G151T, C458T, C496G, A616C, T623C, T742C, T1291C, A1768T, G1858A [Table I (17), (32–35)]. G34A and C421A *BCRP* cDNAs were also used as controls. These *BCRP* germ-line mutations/SNPs have been described previously, some are in publication and the others are in the database of National Center for Biotechnology Information. For the transfection of these *BCRP* cDNA species, we generated bicistronic constructs using the pHa-IRES-DHFR vector. Mutant *BCRP* cDNAs were then prepared using the Mutan-Super Express Km site-directed mutagenesis system (Takara, Ohtsu, Japan) as directed by the manufacturer's instructions. Either wild-type or germ-line mutation/SNP-containing *BCRP* cDNAs without any other mutations were subsequently inserted into the pHa-IRES-DHFR bicistronic retrovirus vector that carries *DHFR* cDNA.

Cell Culture Conditions and Establishment of *BCRP* Transfectants

Murine fibroblast PA317 cells were cultured in Dulbecco's modified eagle medium supplemented with 7% fetal bovine serum at 37°C in a humidified 5% CO_2 environment. For the establishment of both wild-type and mutant *BCRP* transfectants, PA317 cells were transfected with pHa-BCRP-IRES-DHFR constructs containing either wild-type, G34A, G151T, C421A, C458T, A616C, T623C, T742C, T1291C, A1768T, or G1858A *BCRP* cDNA using a MBS Mammalian Transfection Kit (Stratagene, La Jolla, CA). The cells were selected with 120 ng/mL of methotrexate, and the resulting mixed populations of resistant cells were designated as PA/WT, PA/V12M, PA/G51C, PA/Q141K, PA/T153M, PA/I206L, PA/F208S, PA/S248P, PA/F431L, PA/N590Y and PA/D620N, respectively. The PA/F208S clones and PA/F431L clones were obtained by limiting dilution.

Cell Growth Inhibition Assay

Anticancer agent resistance levels in both the parental PA317 cells and in the various BCRP transfectants were

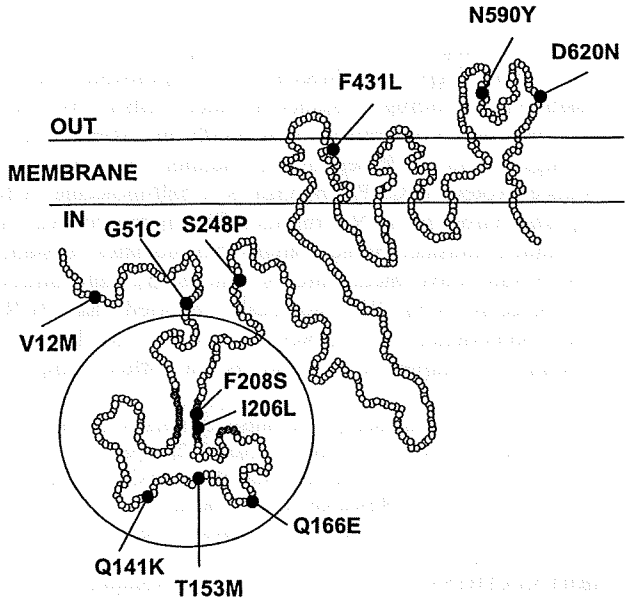

Fig. 1. Schematic representation of the breast cancer resistance protein and locations of the germ-line mutations/SNPs analyzed in this study.

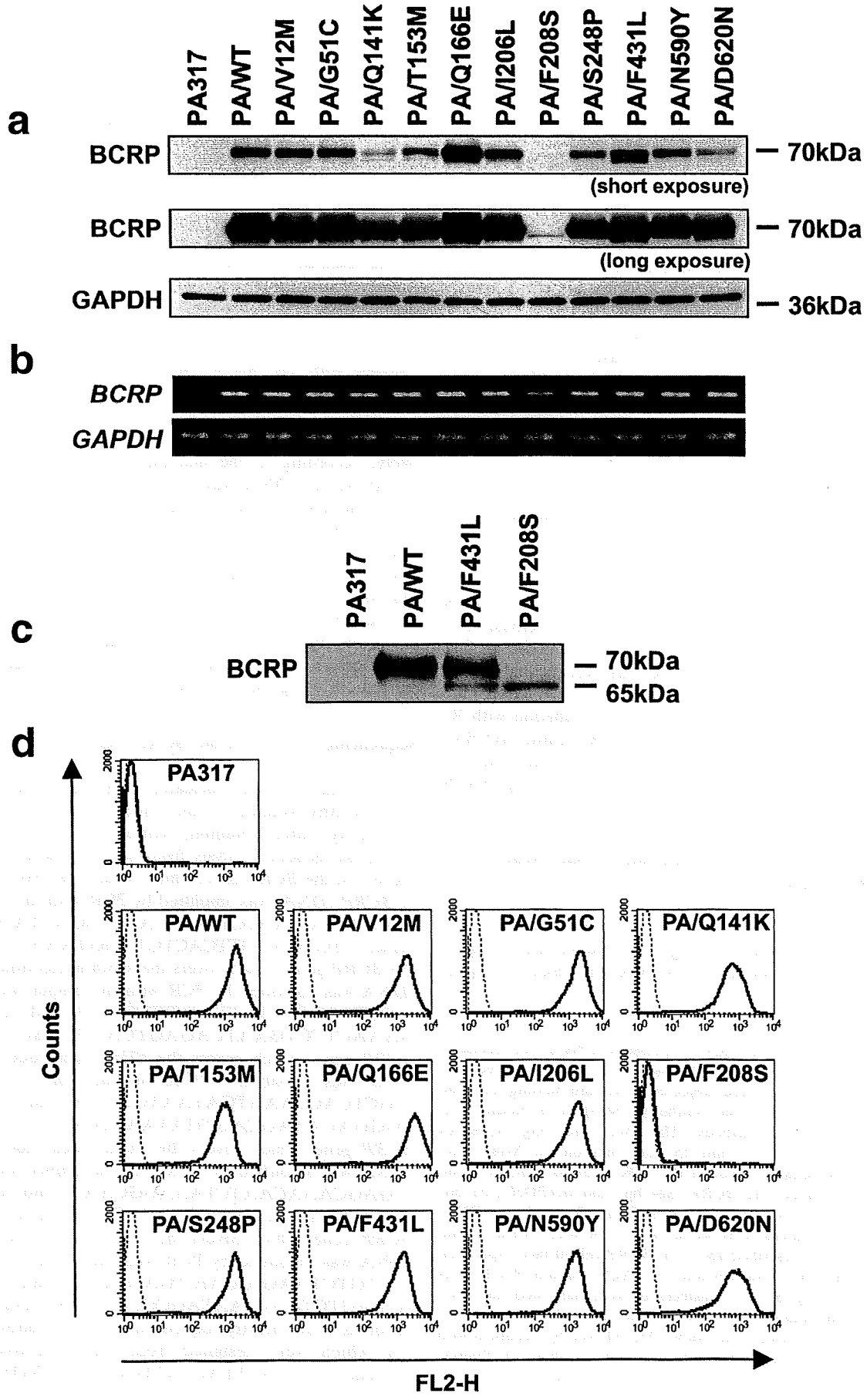
a
PA317
PA/WT
PA/V12M
PA/G51C
PA/Q141K
PA/T153M
PA/Q166E
PA/I206L
PA/F208S
PA/S248P
PA/F431L
PA/N590Y
PA/D620N
BCRP
70kDa
(short exposure)
BCRP
70kDa
(long exposure)
GAPDH
36kDa
b
BCRP
GAPDH
c
PA317
PA/WT
PA/F431L
PA/F208S
BCRP
70kDa
65kDa
d
PA317
PA/WT
PA/V12M
PA/G51C
PA/Q141K
PA/T153M
PA/Q166E
PA/I206L
PA/F208S
PA/S248P
PA/F431L
PA/N590Y
PA/D620N
Counts
FL2-H

evaluated by cell growth inhibition assays after incubation of the cells for 5 days at 37°C in the absence or presence of various concentrations of SN-38 (Yakult Honsha, Tokyo). Cell numbers were determined with a Coulter counter (Sysmex, Kobe, Japan). IC_{50} values (drug dose causing 50% inhibition of cell growth) were determined from growth inhibition curves.

Western Blotting

Cell lysates were obtained as described previously (10). Cell lysates from the *BCRP* transfectants were resolved by SDS-PAGE and then electro-transferred onto a nitrocellulose membrane. The membrane was incubated with 1 μg/mL of anti-BCRP polyclonal antibody 3488 (9) and a GAPDH mouse monoclonal antibody as an internal control, followed by washing and treatment with peroxidase-conjugated sheep anti-rabbit and anti-mouse secondary antibody (Amersham, Buckinghamshire, UK), respectively. The membrane-bound antibodies were visualized with the Enhanced Chemiluminescence (ECL) Plus Western blotting detection system (Amersham).

Fluorescence-activated Cell Sorting (FACS) Analysis of BCRP Expression

The expression levels of human BCRP on the cell surfaces of various *BCRP* transfectants were examined by FACS analysis using a human-specific anti-BCRP monoclonal antibody (eBiosciences, San, Diego, CA), that was raised against a cell surface epitope of BCRP. The cells were incubated with or without a biotinylated anti human ABCG2 (20 μg/mL) for 30 min on ice, followed by washing and incubation with R-phycoerythrin-conjugated streptavidin (400 μg/mL; BD Biosciences, Franklin Lakes, NJ) (20) for 30 min on ice. Fluorescence staining levels were measured using FACS Calibur (BD Biosciences).

Semi-quantitative Reverse Transcriptase Chain Reaction (RT-PCR) Analysis

The isolation of total RNA and subsequent RT-PCR analysis was performed using an RNeasy kit (Qiagen, Valencia, CA) and an RNA LA PCR kit (Takara), respectively, according to the manufacturer's instructions. First-strand *BCRP* cDNA was synthesized from 0.3 μg of total RNA and a 824 bp *BCRP* cDNA fragment was amplified by PCR with the forward and reverse primers, 5′-GATATCAATGATACAGGGTT-3′ and 5′-TGTCCAATAGAATATTCCCC-3′, respectively. The PCR conditions were as follows: 95°C for 5 min, followed by 18–24 cycles of 95°C for 30 sec, 55°C for 30 sec and 72°C for 1 min, and a final extension for 7 min at 72°C. As an internal control, the amplification of *GAPDH* cDNA (551 bp fragment) was carried out using the same procedure.

Table II. SN-38 Resistance Levels of PA317 Transfectants[a]

Cell type	IC_{50} (nmol/L)	Degree of resistance
PA317	11±0.2	1
PA/WT	550±16	50
PA/V12M	490±13	45
PA/Q141K	110±5.9	10
PA/T153M	260±15	24
PA/Q166E	680±40	62
PA/F208S	10±0.7	1
PA/F431L	34±0.9	3
PA/D620N	190±5.7	17

[a] Cells were cultured for 5 days with various concentrations of SN-38. Cell numbers were then measured using a Coulter counter, and the IC_{50} values were determined. The degree of drug resistance is calculated as the IC_{50} ratio of resistant cells divided by that of the parental cells. The data are represented as the mean ± SD from triplicate determinations.

Sequencing Analysis of the *BCRP* Gene

Peripheral blood nucleated cells were obtained from both healthy volunteers and cancer patients of Japanese nationality, after obtaining written informed consent, to undertake genetic analysis from each of these individuals. Exon 2 of the *BCRP* gene, which covers the 151st nucleotide of *BCRP* cDNA, was amplified by PCR with the primer set, forward; 5′-GCAATCTCATTTATCTGGACTA-3′ and reverse; 5′-TGTGAGGTTCACTGTAGGTAAA-3′. Exon 5 of the *BCRP* gene, which covers the 496th nucleotide of *BCRP* cDNA was amplified by PCR with the primer set, forward; 5′-CCTTAGTTATGTTATCTTTGTG-3′ and reverse; 5′-GAAACTTCTGAATCAGAGTCAT-3′. Exon 6 of the *BCRP* gene, which covers the 623rd nucleotide of *BCRP* cDNA was amplified by PCR with the primer set, forward; 5′-GCTCACCAAATGATAATGACT-3′ and reverse; 5′-TGGGACATAGTAGTGATAAGA-3; Exon 7 of the *BCRP* gene, which covers the 742nd nucleotide of *BCRP* cDNA was amplified by PCR with the primer set, forward; 5′-GAGCAAACAATCTAAAGGCAA-3′ and reverse; 5′-ACCCAAAGACCAAACAGCACT-3′. Exon 11 of the *BCRP* gene, which covers the 1291st nucleotide of *BCRP* cDNA was amplified by PCR with the primer set, forward; 5′-CTGTCTAAGAATGCTGAGTTG-3′ and revere; 5′-ATCAGTCTAACCAATAGCCCC-3′. The resulting PCR products were directly sequenced using the following primers, which were designed from the respective intronic sequences; 5′-AACTTACTATTGCTTTTCTGTC-3′ (from

◀ **Fig. 2.** BCRP protein and mRNA expression in PA317 transfectants. **a**, Western blot analysis of BCRP in each of the *BCRP* transfectants. Protein samples (20 μg) were subjected to western blotting using the rabbit anti-BCRP polyclonal antibody (3488) or a mouse anti-GAPDH monoclonal antibody. The short and long exposures indicated were of 5 min and 15 min duration on X-ray film, respectively. **b**, Semi-quantitative RT-PCR of *BCRP* mRNA in the PA317 transfectants. The *BCRP* (824 bp) and *GAPDH* (551 bp) transcripts were amplified by RT-PCR from 0.3 μg of total RNA. **c**, Western blot analysis of BCRP in PA317, PA/WT, PA/F431L, and PA/F208S cells as described above. **d**, BCRP cell surface expression analysis in the PA317 transfectants by FACS. Parental PA317 cells and corresponding *BCRP* transfectants were harvested and then incubated with (*bold line*) or without (*dotted line*) a biotinylated anti-human BCRP monoclonal antibody 5D3, followed by treatment with R-phycoerythrin-conjugated streptavidin. After washing, the fluorescence intensities were measured using FACS Calibur.

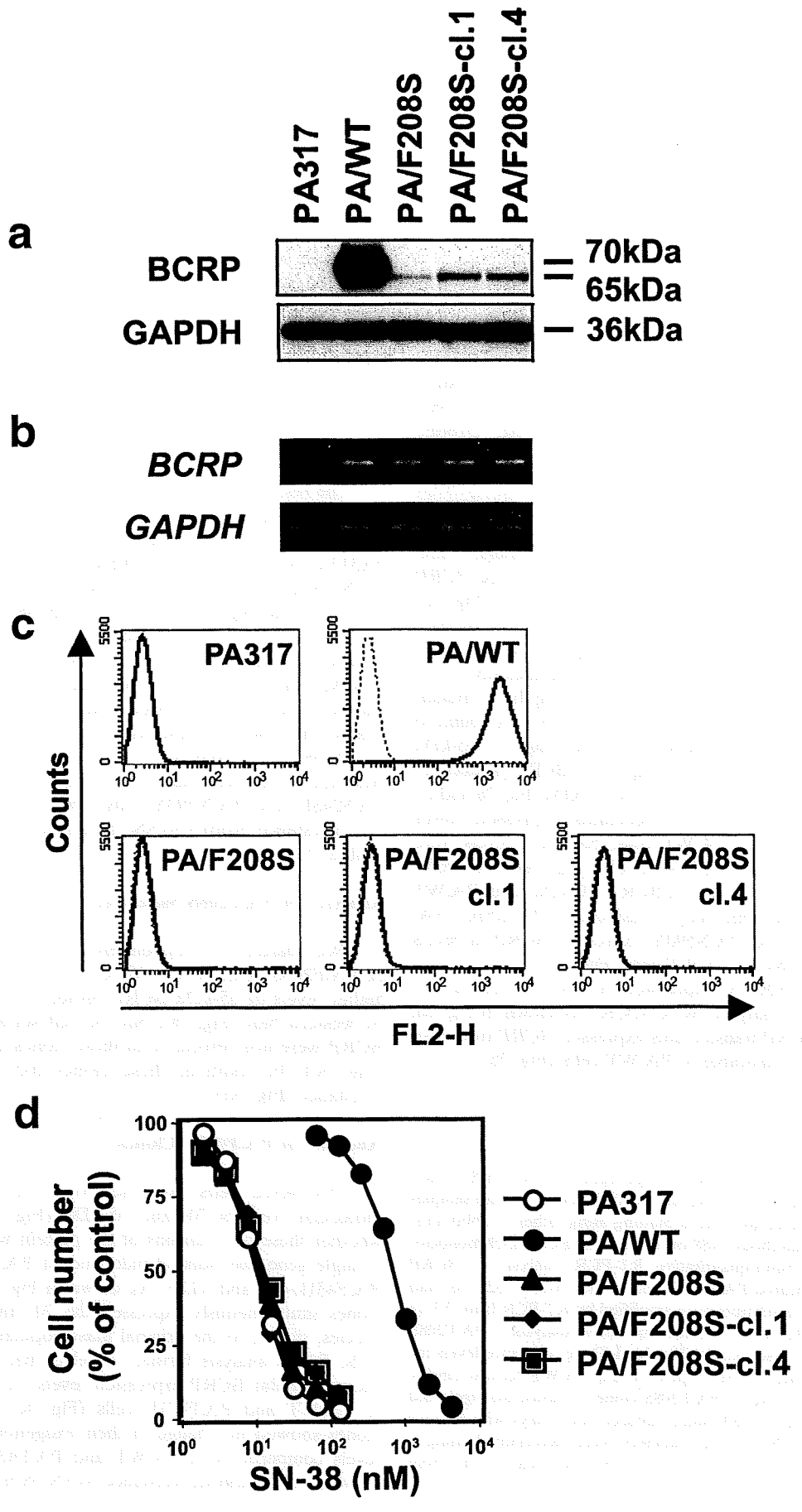
a
PA317
PA/WT
PA/F208S
PA/F208S-cl.1
PA/F208S-cl.4
BCRP
GAPDH
70kDa
65kDa
36kDa
b
BCRP
GAPDH
c
Counts
PA317
PA/WT
PA/F208S
PA/F208S cl.1
PA/F208S cl.4
FL2-H
d
Cell number (% of control)
SN-38 (nM)
PA317
PA/WT
PA/F208S
PA/F208S-cl.1
PA/F208S-cl.4

−46 to −25 upstream of exon 2), 5′-CTAAACAGTCATGGTCTTAGAAA-3′(from −68 to −46 upstream of exon 5), 5′-AAATGATAATGACTGGTTGTT-3′(from −52 to −32 upstream of exon 6), 5′-AAGAATAGAGTATTTTACTGAGA-3′(from −75 to −53 upstream of exon 7), 5′-CTAAGAATGCTGAGTTGACTG-3′(from −50 to −30 upstream of exon 11).

RESULTS

Expression of BCRP in PA317 Transfectants

The germ-line mutations and resulting amino acid substitutions examined in this study were as follows; G151T (G51C), C458T (T153M), C496G (Q166E), A616C (I206L), T623C (F208S), T742C (S248P), T1291C (F431L), A1768T (N590Y) and G1858A (D620N). G51C, T153M, Q166E, I206L, F208S and S248P are located in the intracellular domain of the protein (Fig. 1 and Table I). F431L, N590Y and D620N are located within the transmembrane domain (Fig. 1 and Table I).

BCRP expression levels in each of the PA317 transfectants were then examined by western blotting. The wild-type *BCRP* transfectants (PA/WT) express a 70-kDa BCRP species (Fig. 2a). Similar to previous findings (14), PA/V12M cells were observed to express similar amounts of BCRP compared with PA/WT cells, whereas PA/Q141K cells expressed significantly lower amounts of BCRP than PA/WT (Fig. 2a). Among the 11 mutant BCRP transfectants under study, PA/F208S cells were found to express the lowest levels of BCRP, corresponding to a 65-kDa protein (Fig. 2a and c). PA/F431L expressed BCRP products of two distinct molecular sizes, 70-kDa and 65-kDa (Fig. 2a and c). PA/T153M and PA/D620N transfectants expressed lower amounts of BCRP than PA/WT cells, but these levels were higher than those in the PA/Q141K cells (Fig. 2a). PA/Q166E cells expressed higher amounts of BCRP (70-kDa) than PA/WT cells (Fig. 2a). The remaining transfectants PA/G51C, PA/I206L, PA/S248P, and PA/N590Y expressed BCRP at levels that were comparable to PA/WT cells (Fig. 2a).

The BCRP mRNA expression levels in each of the transfectants were analyzed by RT-PCR. As shown in Fig. 2b, the 11 mutant *BCRP* transfectants expressed *BCRP* transcript levels that were comparable to PA/WT cells (Fig. 2b).

◀ **Fig. 3.** BCRP protein and mRNA expression in PA/F208S clones. **a**, Western blot analysis of BCRP in PA/208S clones. Protein samples (20 μg) were subjected to western blotting using either a rabbit anti-BCRP polyclonal antibody 3488 or a mouse anti-GAPDH monoclonal antibody. **b**, Semi-quantitative RT-PCR analysis of *BCRP* mRNA in the indicated PA/F208S clones. The *BCRP* (824 bp) and *GAPDH* (551 bp) transcripts were amplified by RT-PCR from 0.3 μg of total RNA. **c**, BCRP cell surface expression analysis of PA/F208S clones by FACS as described for Fig. 2d. **d**, Drug resistance levels for the PA/F208S clones. PA317 (*open circle*), PA/WT (*closed circle*), PA/F208S (*closed triangle*), PA/F208S clone 1 (*closed lozenge*), and clone 4 (*closed square*) cells were cultured for 5 days with various concentrations of SN-38. Cell numbers were determined using a Coulter counter. Data are represented by the mean ± SD from triplicate experiments.

Cell Surface BCRP Expression in the Mutant *BCRP* Transfectants

The expression levels of BCRP on the cell surfaces of each of the transfectants were examined by FACS and were undetectable in either the PA/F208S or parental PA317 cells (Fig. 2d). PA/Q141K, PA/T153M and PA/D620N cells expressed lower amounts of BCRP on their cell surfaces than PA/WT cells (Fig. 2d). These results were consistent with the immunoblotting analysis (Fig. 2a). The cell surface expression of BCRP in PA/Q166E cells was slightly higher compared with PA/WT cells (Fig. 2d). Each of the other transfectants (PA/G51C, PA/I206L, PA/S248P, PA/F431L, and PA/N590Y cells) showed similar cell surface BCRP expression levels to PA/WT (Fig. 2d).

Drug Resistance of Mutant *BCRP* Transfectants

The resistance of each of the *BCPR* transfectants to SN-38 was analyzed by cell growth inhibition assay. PA/WT cells showed a 50-fold higher resistance to SN-38 than the parental PA317 cells (Table II). PA/F208S cells showed a similar level of SN-38 sensitivity to PA317 cells (Table II). PA/F431L cells showed 3-fold higher resistance to SN-38 than PA317 cells but PA/F431L cells were found to be 15-fold more sensitive to this agent than PA/WT cells (Table II). PA/Q141K, PA/T153M, and PA/D620N cells showed 10–24-fold higher resistance levels to SN-38 compared with the parental cells (Table II). However, these cells were 2–5 times more sensitive to SN-38 when compared with PA/WT cells (Table II). Additional transfectants (PA/G51C, PA/Q166E, PA/I206L, PA/S248P, and PA/N590Y cells) showed no change in their drug resistance profiles to SN-38 compared with PA/WT cells (Table II).

Analyses of PA/F208S Subclones

We isolated two independent clones from the population of PA/F208S cells, (PA/F208S-cl.1 and -cl.4) that expressed higher levels of 65-kDa BCRP protein than PA/F208S cells by western blot (Fig. 3a), but the cell surface expression of BCRP were not detectable in these clones by FACS analysis (Fig. 3c). In addition, these clones did not show SN-38 resistance (Fig. 3d).

Analyses of PA/F431L Clones

PA/F431L cells expressed two species of BCRP of molecular weights 70- and 65-kDa (Fig. 2a). To confirm whether these two versions of the protein were derived from a single gene, we isolated independent PA/F431L subclones, PA/F431L-cl.6 and -cl.15. As shown in Fig. 4a, both of these clones simultaneously expressed the 70- and 65-kDa BCRP species, similar to the original mass population of PA/F431L cells. FACS analysis further revealed that these clones also showed similar BCRP expression levels on their cell surfaces to PA/WT and PA/F431L cells (Fig. 4c). Moreover, these clones showed no change in their exogenous *BCRP* mRNA levels compared with PA/WT and PA/F431L (Fig. 4b) but showed only marginal resistance to SN-38 treatment (Fig. 4d).

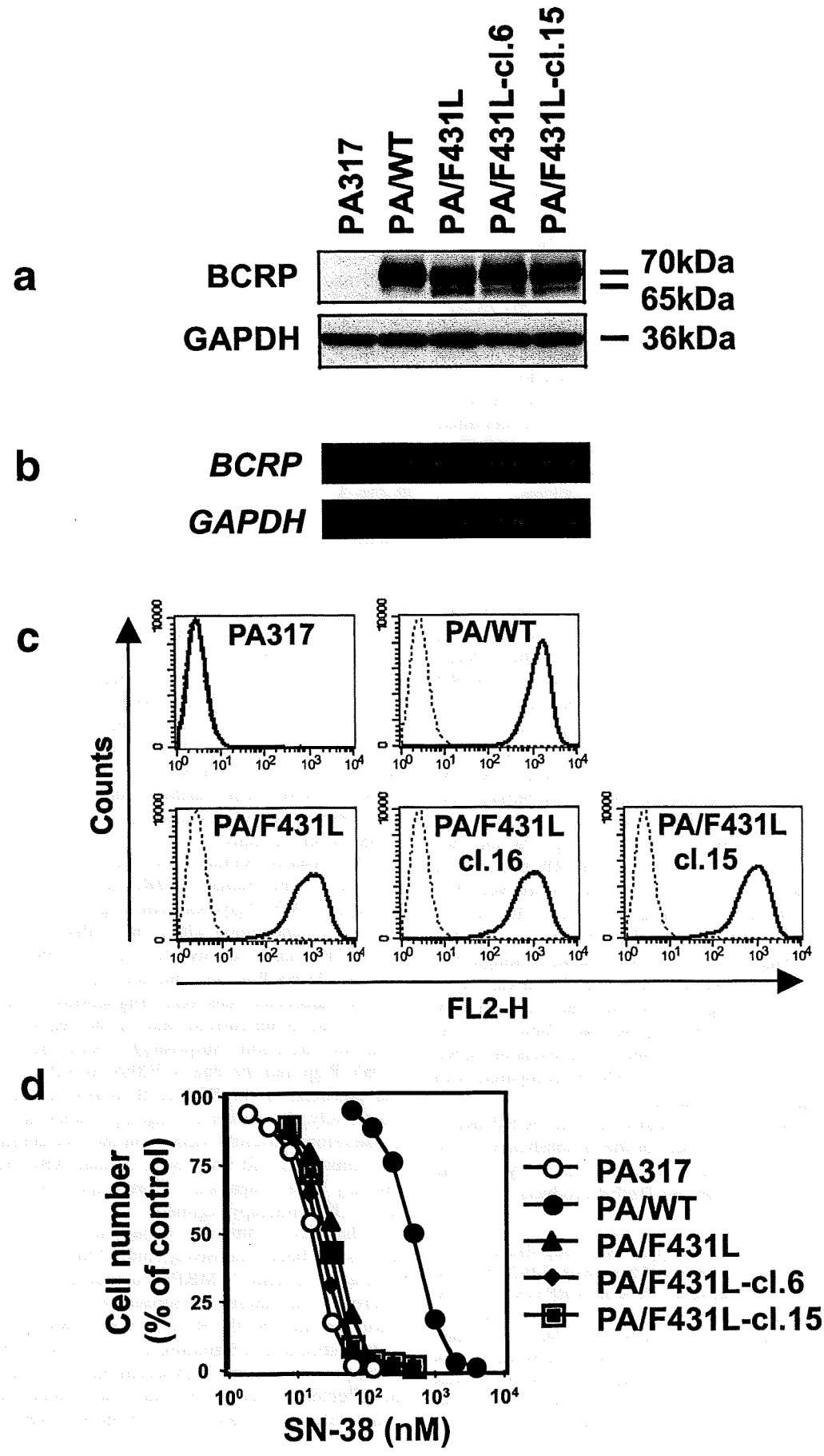
a
PA317
PA/WT
PA/F431L
PA/F431L-cl.6
PA/F431L-cl.15
BCRP
GAPDH
70kDa
65kDa
36kDa
b
BCRP
GAPDH
c
PA317
PA/WT
PA/F431L
PA/F431L cl.16
PA/F431L cl.15
Counts
FL2-H
d
Cell number (% of control)
SN-38 (nM)
PA317
PA/WT
PA/F431L
PA/F431L-cl.6
PA/F431L-cl.15

Frequencies of Germ-line Mutations Within the *BCRP* Gene

Due to the possible significance of the T623C and T1291C *BCRP* mutations, we examined the frequencies of five germ-line mutations, G151T, C496G, T623C, T742C and T1291C *BCRP*, among Japanese populations. We analyzed 200–350 samples in this study, depending on the frequency of each mutation. As shown in Table I, allele frequencies for the T623C *BCRP* and T1291C *BCRP* allele were 0.3% and 0.6%, respectively. A healthy volunteer was heterozygous for the T623C *BCRP* allele. Two healthy volunteer and a cancer patient were heterozygous for the T1291C *BCRP* allele. We previously reported that allele frequency for the C376T *BCRP*, that encodes a truncated protein, was 1.2% in the Japanese population (17). From both our previous and present results, we conclude that there are in fact two non-functional germ-line mutations/SNPs in the *BCRP* gene, C376T and T623C. It should be noted however that we have not thus far identified any individuals who are homozygous for either the C376T or T623C alleles, nor have we observed individuals who are heterozygous for a combination of these two alleles.

DISCUSSION

In our current study, we have examined the effect of the nine germ-line mutations/SNPs, G151T, C458T, C496G, A616C, T623C, T742C, T1291C, A1768T, and G1858A *BCRP*, resulting in the amino acid changes G51C, T153M, Q166E, I206L, F208S, S248P, F431L, N590Y, D620N, respectively, on BCRP protein expression and function. We first obtained both the wild-type and mutant *BCRP* cDNAs and expressed each in PA317 cells. The resulting mixed populations of cells were designated a PA/WT, PA/V12M, PA/G51C, PA/Q141K, PA/T153M, PA/I206L, PA/F208S, PA/S248P, PA/F431L, PA/N590Y and PA/D620N. PA/F208S cells were found to express marginal levels of BCRP (65-kDa) (Figs. 2a and 3a), which were slightly lower than wild-type BCRP, but did not appear on the cell surface (Figs. 2d and 3c). Moreover, PA/F208S cells did not show any drug resistance (Fig. 3c and Table II). PA/F431L cells expressed a 65-kDa and 70-kDa species of BCRP (Figs. 2a and 4a). In addition, although PA/F431L cells expressed BCRP at cell surface levels that were similar to PA/WT cells (Figs. 2d and 4c), they showed only marginal resistance to SN-38 (Fig. 4d and Table II). PA/T153M and PA/D620N cells expressed lower levels of BCRP and also showed lower resistance to SN-38, compared with PA/WT cells (Fig. 2a and Table II).

Our previously described bicistronic pHa-BCRP-IRES-DHFR construct (20–23) was used for the establishment of the mutant *BCRP* transfectants in the present study. In the resulting transfectants, *BCRP* and *DHFR* products are translated independently from single bicistronic mRNAs that are transcribed under the control of a retroviral long terminal repeat promoter. The upstream *BCRP* cDNA is translated in a cap-dependent manner, and the downstream *DHFR* is translated under the control of the IRES. Hence, cells expressing *DHFR*, resulting in methotrexate resistance, theoretically always coexpress the *BCRP* cDNA. It is noteworthy that methotrexate itself is reported to be a substrate of BCRP (24,25), but wild-type BCRP-transfected cells show only marginal resistance to this drug. In addition, BCRP expression does not affect the survival of cells transfected with the bicistronic DHFR vector, and mixed population of the methotrexate-resistant colonies (>100) were used in this study.

The amino acid positions of the germ-line mutations/SNPs examined in this study are represented by the black circles in Fig. 1. G51C, T153M, Q166E, I206L, F208S, and S248P are located in the intracellular domain, and F431L, N590Y, and D620N reside in the transmembrane domain. Walker A (80–89), Walker B (204–210), and Signature C (186–190) in the ATP binding site of BCRP are indicated by the gray circles in Fig. 1 and are conserved in other members of the ATP transporter family (26). The I206L BCRP and F208S BCRP mutants harbor amino acid substitutions within the Walker B region, which is likely to have a significant impact upon the functioning of the ATP binding site. PA/F208S cells express a marginal amount of a smaller BCRP protein species(65 kDa), which is not expressed on the cell surface (Figs. 2a, c, d, 3a and c). Moreover, PA/F208S cells do not show any drug resistant properties. Considering no expression of F208S BCRP mutant on the cell surface of PA/F208S, the lack of drug resistance property in the transfectant is probably due to the absence of cell surface transporter. On the other hand, PA/I206L cells show similar levels of BCRP expression and the resistance to SN-38 as PA/WT cells. Further studies are ongoing to evaluate the ATP-binding and -hydrolyzing activity of I206L BCRP and F208S BCRP mutants.

We recently examined the effects of a T3587G germ-line mutation in the human *MDR1* gene and found that the resulting I1196Y P-glycoprotein (P-gp), that also contains an amino acid substitution within the Walker B domain, did not have ATP-binding activity (27). In our T3587G *MDR1* transfectants, I1196S P-gp also did not appear on the cell surface, and the transfected cells were drug sensitive. These results are very similar to our current data for the T623C (F208S) *BCRP* germ-line mutation. Surprisingly, both the Ile residue of I1196Y P-gp and the Phe of F208S BCRP occupy the amino acid positions in the Walker B motifs of P-gp and BCRP, respectively. A number of ongoing studies in our laboratory are therefore currently focused on the mechanisms underlying the maturation and stability of mutant ABC transporters as this may have a significant impact upon the effectiveness of cancer chemotherapy regimens.

The loss of function of particular mutant ABC transporters has been extensively studied for multidrug resistance associated protein 2 (MRP2) in relation to Dubin-Johnson syndrome, an inherited disorder defined by chronic hyperbilirubinemia (28–30). R768W MRP2, which has the amino acid substitution in Signature C of the first ATP binding site of the protein, confers high serum bilirubin concentrations in the affected patients (28), and the mutant protein is not completely glycosylated (29). Q1382R MRP2 is a mutation

◀ **Fig. 4.** BCRP protein and mRNA expression in PA/F431L clones as described in Figs. 2 and 3. **a**, Western blot analysis of BCRP in PA/F431L clones **b**, Semi-quantitative RT-PCR of *BCRP* mRNA in PA/F431L clones. **c**, BCRP cell surface expression analysis of PA/F431L clones by FACS. **d**, Drug resistance levels in the PA/F431L clones. PA317 (*open circle*), PA/WT (*closed circle*), PA/F431L (*closed triangle*), PA/F431L clone 6 (*closed lozenge*), and PA/F431L clone 15 (*closed square*) cells were cultured for 5 days with various concentrations of SN-38 and assayed as described in Fig. 3d.

between the Walker A and the Signature C regions of the second ATP-binding site, and causes loss of ATP hydrolysis activity (29). Furthermore, the deletion of Arg-1392 and Met-1393 in MRP2, located between the Walker A and the Signature C regions of the second ATP-binding site, leads to both impaired maturation and trafficking of the protein (30). Based upon these earlier reports, it is evident that various amino acid substitutions in the ATP binding domain can result in a dysfunctional ABC transporter.

The F431L residue is located in the second transmembrane domain (Fig. 1) and PA/F431L cells express two species of BCRP of 70-kDa and 65-kDa in size. The 65-kDa F431L BCRP product has the same molecular weight as F208S BCRP by SDS-PAGE (Fig. 2a and c). From the results of our analysis of PA/F431L clones, these two products seemed to be generated from a single cDNA species (Fig. 4b). The 70-kDa BCRP expression levels in PA/F431L cells were also much higher than the 65-kDa BCRP protein in the same cells (Figs. 2c and 4c). Although PA/F431L cells express higher quantities of 70-kDa BCRP compared with PA/Q141K, PA/T153M, and PA/D620N cells (Fig. 2a) these cells in fact show a lower resistance to SN-38 than these other three transfectants (Table II). From these results, we speculate that this residue might in fact be important in the recognition of SN-38, and that the F431L substitution may result in lower transporter function than the wild-type protein. We previously reported that seven mutants of BCRP at residue E446, located in the second transmembrane domain, did not show any drug resistance and that 13 mutants of BCRP at R482, residing in the third transmembrane domain, showed higher resistance to mitoxantron and doxorubicin than wild-type BCRP (31).

PA/T153M and PA/D620N cells showed low-levels of BCRP expression and drug resistance to SN-38 compared with PA/WT cells (Fig. 2a and Table II). These results were similar to the data obtained for PA/Q141K cells and based upon these data, we hypothesize that the decrease in the resistance levels to SN-38 may not be due to functional alterations but to decreased protein expression. Similar results were obtained using NIIH3T3/T153M and NIH3T3/D620N cells (date not shown).

The possible significance of the C421A *BCRP* was recently evaluated in a phase I study of diflomotecan, a new camptothecin derivative anticancer drug (18). In this study, five patients who were heterozygous for the C421A allele showed three-fold higher blood drug concentrations of diflomotecan than 15 patients who had wild-type allele (18). Following intravenous administration of this drug, the area-under-curve (AUC) of the individuals with the C421A allele and patients who were homozygous wild-type were 138 ng·h/mL and 46.1 ng·h/mL, respectively ($P = 0.015$). This study has therefore clearly shown that germ-line mutations/SNPs in the *BCRP* gene that cause a reduction in expression or loss of functions of the protein will alter the pharmacokinetics of BCRP substrate anticancer agents.

CONCLUSION

We have characterized two important *BCRP* germ-line mutations, T623C (F208S) and T1291C (F431L). T623C *BCRP* cDNA encodes a non-functional BCRP, and T1291C *BCRP* cDNA encodes a low-functional protein product. Polymorphisms within the *BCRP* genes of individuals that severely disrupt transporter activity are thus likely to be associated with hypersensitivity to substrate anticancer agents. Because BCRP may play crucial roles in the absorption and excretion of anticancer drugs, the monitoring of *BCRP* germ-line mutations/SNPs should be considered carefully during the clinical development of novel anticancer agents and BCRP-reversing drugs.

ACKNOWLEDGMENTS

This study was supported by the Ministry of Education, Culture, Sports, Science and Technology, and the Ministry of Health, Labor and Welfare, Japan.

REFERENCES

1. M. M. Gottesman, C. A. Hrycyna, P. V. Schoenlein, U. A. Germann, and I. Pastan. Genetic analysis of the multidrug transporter. *Annu. Rev. Genet.* **29**:607–649 (1995).
2. C. J. Chen, J. E. Chin, K. Ueda, D. P. Clark, I. Pastan, M. M. Gottesman, and I. B. Roninson. Internal duplication and homology with bacterial transport proteins in the mdr1 (P-glycoprotein) gene from multidrug-resistant human cells. *Cell* **47**:381–389 (1986).
3. S. P. Cole, G. Bhardwaj, J. H. Gerlach, J. E. Mackie, C. E. Grant, K. C. Almquist, A. J. Stewart, E. U. Kurz, A. M. Duncan, and R. G. Deeley. Overexpression of a transporter gene in a multidrug-resistant human lung cancer cell line. *Science* **258**:1650–1654 (1992).
4. R. Allikmets, L. M. Schriml, A. Hutchinson, V. Romano-Spica, and M. Dean. A human placenta-specific ATP-binding cassette gene (ABCP) on chromosome 4q22 that is involved in multidrug resistance. *Cancer Res.* **58**:5337–5339 (1998).
5. L. A. Doyle, W. Yang, L. V. Abruzzo, T. Krogmann, Y. Gao, A. K. Rishi, and D. D. Ross. A multidrug resistance transporter from human MCF-7 breast cancer cells. *Proc. Natl. Acad. Sci. U.S.A.* **95**:15665–15670 (1998).
6. K. Miyake, L. Mickley, T. Litman, Z. Zhan, R. Robey, B. Cristensen, M. Brangi, L. Greenberger, M. Dean, T. Fojo, and S. E. Beates. Molecular cloning of cDNAs which are highly overexpressed in mitoxantrone-resistant cells: demonstration of homology to ABC transport genes. *Cancer Res.* **59**:8–13 (1999).
7. M. Maliepaard, M. A. van Gastelen, L. A. de Jong, D. Pluim, R. C. van Waardenburg, M. C. Ruevekamp-Helmers, B. G. Floot, and J. H. Schellens. Overexpression of the BCRP/MXR/ABCP gene in a topotecan-selected ovarian tumor cell line. *Cancer Res.* **59**:4559–4563 (1999).
8. S. Kawabata, M. Oka, K. Shiozawa, K. Tsukamoto, K. Nakatomi, H. Soda, M. Fukuda, Y. Ikegami, K. Sugahara, Y. Yamada, S. Kamihira, L. A. Doyle, D. D. Ross, and S. Kohno. Breast cancer resistance protein directly confers SN-38 resistance of lung cancer cells. *Biochem. Biophys. Res. Commun.* **280**:1216–1223 (2001).
9. K. Kage, S. Tsukahara, T. Sugiyama, S. Asada, E. Ishikawa, T. Tsuruo, and Y. Sugimoto. Dominant-negative inhibition of breast cancer resistance protein as drug efflux pump through the inhibition of S-S dependent homodimerization. *Int. J. Cancer* **97**:626–630 (2002).
10. K. Kage, T. Fujita, and Y. Sugimoto. Role of Cys-603 in dimer/oligomer formation of the breast cancer resistance protein BCRP/ABCG2. *Cancer Sci.* **96**:866–872 (2005).
11. Y. Imai, S. Asada, S. Tsukahara, E. Ishikawa, T. Tsuruo, and Y. Sugimoto. Breast cancer resistance protein exports sulfated estrogens but not free estrogens. *Mol. Pharmacol.* **64**:610–618 (2003).
12. M. Maliepaard, G. L. Scheffer, I. F. Faneyte, M. A. Gastelenvan, A. C. Pijnenborg, A. H. Schinkel, M. J. Vijvervan De, R. J. Scheper, and J. H. Schellens. Subcellular localization and distribution of the breast cancer resistance protein transporter in normal human tissues. *Cancer Res.* **61**:3458–3464 (2001).
13. S. Zhou, J. D. Schuetz, K. D. Bunting, A. M. Colapietro, J. Sampath, J. J. Morris, I. Lagutinal, G. C. Grosveld, M. Osawa,

H. Nakauchi, and B. P. Sorrentino. The ABC transporter Bcrp1/ABCG2 is expressed in a wide variety of stem cells and is a molecular determinant of the side-population phenotype. *Nat. Med.* **7**:1028–1034 (2001).
14. D. M. Kolkvan der, E. Vellenga, G. L. Scheffer, M. Muller, S. E. Bates, R. J. Scheper, and E. G. Vriesde. Expression and activity of breast cancer resistance protein (BCRP) in de novo and relapsed acute myeloid leukemia. *Blood* **99**:3763–3770 (2002).
15. M. M. van den Heuvel-Eibrink, E. A. Wiemer, A. Prins, J. P. Meijerink, P. J. Vossebeld, B. van der Holt, R. Pieters, P. Sonneveld. Increased expression of the breast cancer resistance protein (BCRP) in relapsed or refractory acute myeloid leukemia (AML). *Leukemia* **16**:833–839 (2002).
16. J. W. Jonker, G. Merino, S. Musters, A. E. van Herwaarden, E. Bolscher, E. Wagenaar, E. Mesman, T. C. Dale, and A. H. Schinkel. The breast cancer resistance protein BCRP (ABCG2) concentrates drugs and carcinogenic xenotoxins into milk. *Nat. Med.* **11**:127–129 (2005).
17. Y. Imai, M. Nakane, K. Kage, S. Tsukahara, E. Ishikawa, T. Tsuruo, Y. Miki, and Y. Sugimoto. C421A polymorphism in the human breast cancer resistance protein gene is associated with low expression of Q141K protein and low-level drug resistance. *Mol. Cancer Ther.* **1**:611–616 (2002).
18. A. Sparreboom, H. Gelderblom, S. Marsh, R. Ahluwalia, R. Obach, P. Principe, C. Twelves, J. Verweij, and H. L. Mcleod. Diflomotecan pharmacokinetics in relation to ABCG2 421C>A genotype. *Clin. Pharmacol. Ther.* **76**:38–44 (2004).
19. W. Zhang, B. N. Yu, Y. J. He, L. Fan, Q. Li, Z. Q. Liu, A. Wang, Y. L. Liu, Z. R. Tan, Fen-Jiang, Y. F. Huang, and H. H. Zhou. Role of BCRP 421C>A polymorphism on rosuvastatin pharmacokinetics in healthy Chinese males. *Clin. Chim. Acta* **373**:99–103 (2006).
20. Y. Sugimoto, S. Tsukahara, S. Sato, M. Suzuki, H. Nunoi, H. L. Malech, M. M. Gottesman, and T. Tsuruo. Drug-selected coexpression of P-glycoprotein and gp91 *in vivo* from an MDR1-bicistronic retrovirus vector Ha-MDR-IRES-gp91. *J. Gene Med.* **5**:366–376 (2003).
21. Y. Sugimoto, I. Aksentijevich, M. M. Gottesman, and I. Pastan. Efficient expression of drug-selectable genes in retroviral vectors under control of an internal ribosome entry site. *Biotechnology (N Y)* **12**:694–698 (1994).
22. Y. Sugimoto, C. A. Hrycyna, I. I. Aksentijevich, I. I. Pastan, and M. M. Gottesman. Coexpression of a multidrug-resistance gene (MDR1) and herpes simplex virus thymidine kinase gene as part of a bicistronic messenger RNA in a retrovirus vector allows selective killing of MDR1-transduced cells. *Clin. Cancer Res.* **1**:447–457 (1995).
23. Y. Sugimoto, S. Sato, S. Tsukahara, M. Suzuki, E. Okochi, M. M. Gottesman, I. Pastan, and T. Tsuruo. Coexpression of a multidrug resistance gene (MDR1) and herpes simplex virus thymidine kinase gene in a bicistronic retroviral vector Ha-MDR-IRES-TK allows selective killing of MDR1-transduced human tumors transplanted in nude mice. *Cancer Gene Ther.* **4**:51–58 (1997).
24. Z. S. Chen, R. W. Robey, M. G. Belinsky, I. Shchaveleva, X. Q. Ren, Y. Sugimoto, D. D. Ross, S. E. Bates, and G. D. Kruh. Transport of methotrexate, methotrexate polyglutamates, and 17beta-estradiol 17-(beta-D-glucuronide) by ABCG2: effects of acquired mutations at R482 on methotrexate transport. *Cancer Res.* **63**:4048–4054 (2003).
25. E. L. Volk, K. M. Farley, Y. Wu, F. Li, R. W. Robey, and E. Schneider. Overexpression of wild-type breast cancer resistance protein mediates methotrexate resistance. *Cancer Res.* **62**: 5035–5040 (2002).
26. L. F. Payen, M. Gao, C. J. Westlake, S. P. Cole, and R. G. Deeley. Role of carboxylate residues adjacent to the conserved core Walker B motifs in the catalytic cycle of multidrug resistance protein 1 (ABCC1). *J. Biol. Chem.* **278**:38537–38547 (2003).
27. K. Mutoh, J. Mitsuhashi, Y. Kimura, S. Tsukahara, E. Ishikawa, K. Sai, S. Ozawa, J. Sawada, K. Ueda, K. Katayama, and Y. Sugimoto. A T3587G germ-line mutation of the MDR1 gene encodes a nonfunctional P-glycoprotein. *Mol. Cancer Ther.* **5**:877–884 (2006).
28. M. Wada, S. Toh, K. Taniguchi, T. Nakamura, T. Uchiumi, K. Kohno, I. Yoshida, A. Kimura, S. Sakisaka, Y. Adachi, and M. Kuwano. Mutations in the canilicular multispecific organic anion transporter (cMOAT) gene, a novel ABC transporter, in patients with hyperbilirubinemia II/Dubin-Johnson syndrome. *Hum. Mol. Genet.* **7**:203–207 (1998).
29. K. Hashimoto, T. Uchiumi, T. Konno, T. Ebihara, T. Nakamura, M. Wada, S. Sakisaka, F. Maniwa, T. Amachi, K. Ueda, and M. Kuwano. Trafficking and functional defects by mutations of the ATP-binding domains in MRP2 in patients with Dubin-Johnson syndrome. *Hepatology* **36**:1236–1245 (2002).
30. V. Keitel, J. Kartenbeck, A. T. Nies, H. Spring, M. Brom, and D. Keppler. Impaired protein maturation of the conjugate export pump multidrug resistance protein 2 as a consequence of a deletion mutation in Dubin-Johnson syndrome. *Hepatology* **32**:1317–1328 (2000).
31. M. Miwa, S. Tsukahara, E. Ishikawa, S. Asada, Y. Imai, and Y. Sugimoto. Single amino acid substitutions in the transmembrane domains of breast cancer resistance protein (BCRP) alter cross resistance patterns in transfectants. *Int. J. Cancer* **107**:757–763 (2003).
32. S. Mizuarai, N. Aozasa, and H. Kotani. Single nucleotide polymorphisms result in impaired membrane localization and reduced atpase activity in multidrug transporter ABCG2. *Int. J. Cancer* **109**:238–246 (2004).
33. C. P. Zamber, J. K. Lamba, K. Yasuda, J. Farnum, K. Thummel, J. D. Schuetz, and E. G. Schuetz. Natural allelic variants of breast cancer resistance protein (BCRP) and their relationship to BCRP expression in human intestine. *Pharmacogenetics* **13**:19–28 (2003).
34. M. Itoda, Y. Saito, K. Shirao, H. Minami, A. Ohtsu, T. Yoshida, N. Saijo, H. Suzuki, Y. Sugiyama, S. Ozawa, and J. Sawada. Eight novel single nucleotide polymorphisms in ABCG2/BCRP in Japanese cancer patients administered irinotacan. *Drug Metab. Pharmacokinet.* **18**:212–217 (2003).
35. Y. Honjo, K. Morisaki, L. M. Huff, R. W. Robey, J. Hung, M. Dean, and S. E. Bates. Single-nucleotide polymorphism (SNP) analysis in the ABC half-transporter ABCG2 (MXR/BCRP/ABCP1). *Cancer Biol. Ther.* **1**:696–702 (2002).